UNIVERSITY OF CALIFORNIA,
IRVINE

Electrophysiological Studies of Visual Attention and of Emotion Regulation

DISSERTATION

submitted in partial satisfaction of the requirements
for the degree of

DOCTOR OF PHILOSOPHY

in Psychology with concentration in Cognitive Neuroscience

by

Veronica C. Chu

Dissertation Committee:
Professor Michael D'Zmura, Chair
Professor Ramesh Srinivasan
Professor Charles E. (Ted) Wright

2019

Table of Contents

List of Figures

List of Tables

Acknowledgements

I would like to express my gratitude and appreciation to my committee chair and advisor, Professor Michael D'Zmura. Without his guidance and support throughout the past five years, this dissertation would not have been possible.

I would like to thank my committee members, Professor Ramesh Srinivasan and Professor Ted Wright, and members of my advancement to candidacy committee, Professor Jeff Krichmar and Assistant Professor Beth Lopour, for their invaluable comments and suggestions.

I would also like to thank Dr. Jonathan Gratch and Dr. Peter Khooshabeh for the opportunity to work with them at USC Institute of Creative Technologies and their support in the third chapter of this dissertation.

In addition, I would like to thank my former and current colleagues of the Cognitive Neurosystems Lab. Each member provided academic support through advice, feedback, and participation in experiments. Their support helped bring this dissertation to life.

Curriculum Vitae

Veronica Chu

2013	B.A. in Psychology and Philosophy, University of Southern California
2014-2018	Teaching Assistant, Department of Cognitive Sciences, University of California, Irvine
2014-2019	Graduate Student Researcher, Department of Cognitive Sciences, University of California, Irvine
2016	M.S. in Cognitive Neuroscience, University of California, Irvine
2016	Visiting Research Assistant, USC Institute of Creative Technologies
2018	Visiting Researcher, U.S. Army Research Laboratory
2019	Ph.D. in Psychology with concentration in Cognitive Neuroscience, University of California, Irvine

FIELD OF STUDY

Cognitive Science

PUBLICATIONS

Chu, V. C., Lucas, G. M., Lei, S., Mozgai, S., Khooshabeh, P., & Gratch, J. (2019). Emotion regulation in the Prisoner's Dilemma: Effects of reappraisal on behavioral measures and cardiovascular measures of challenge and threat. *Frontiers in Human Neuroscience*. doi: 10.3389/fnhum.2019.00050

Chu, V. C. and D'Zmura, M. (2019). Tracking Feature-Based Attention. *Journal of Neural Engineering*. doi: 10.1088/1741-2552/aaed17

Johnson, K., Iyer, R., Wojcik, S., Vaisey, S., Miles, A., Chu, V., & Graham, J. Ideology-Specific Patterns of Moral Indifference Predict Intentions Not to Vote. *Analyses of Social Issues and Public Policy*. doi: 10.1111/asap.12039

Abstract of the Dissertation

Electrophysiological Studies of Visual Attention and of Emotion Regulation

By

Veronica Chu

Doctor of Philosophy in Psychology

University of California, Irvine, 2019

Professor Michael D'Zmura, Chair

Electrophysiological methods, such as electroencephalography (EEG) and electrocardiography (ECG), measure biological activity that allow us to infer underlying cognitive processes. In the first study, we use EEG to track feature-based attention (FBA), a form of visual attention that helps one detect objects with a particular color, motion, or orientation. We explore the use of SSVEPs, generated by flicker presented peripherally, to track attention in a visual search task presented centrally. Classification results show that one can track an observer's attended color, which suggests that these methods may provide a viable means for tracking FBA in a real-time task. In the second study, we use cardiovascular measures to examine influences of the emotion regulation strategy of reappraisal. We examine cooperation and cardiovascular responses in individuals that were defected on by their opponent in the first round of an iterated Prisoner's Dilemma. We find significant differences between the emotion regulation conditions using the biopsychosocial (BPS) model of challenge and threat, where participants primed with the reappraisal strategy were weakly comparable with a threat state of the BPS model and participants without an emotion regulation were weakly comparable with a challenge state of the BPS model. In the third study, we use EEG to study the chromatic sensitivity of FBA for color during a visual search task. We use SSVEP responses evoked through peripheral flicker to measure the spectral tuning of color detection mechanisms and how attentional selection is affected by distractor color. Our results find smaller responses for the distractor colors and suggest that feature-based attention to a particular color involves chromatic mechanisms that both enhance the response to a target and minimize responses to distractors.

1 Introduction

Chapter 2 discusses an experiment aimed at tracking feature-based attention in a virtual environment using a peripherally flickering stimulus to evoke electrophysiological activity in the brain. Chapter 3 discusses an experiment aimed at studying the effects of emotion regulation on behavioral and cardiovascular measures. Chapter 4 discusses an experiment aimed at studying feature-based attentional filters manipulated by surrounding distractors, measured using peripherally flicker stimuli to evoke electrophysiological activity.

2 Tracking Feature-Based Attention

This study was published in *Journal of Neural Engineering* at https://doi.org/10.1088/1741-2552/aaed17

2.1 Introduction

Electrophysiological and neuroimaging studies have explored attentional mechanisms that help us select for detailed processing those elements of complex visual scenes that are most likely to be useful in a given task. For spatial attention, these studies have found increased neural activity when attention is directed at a region of space (Morgan, Hansen, & Hillyard, 1996; N. G. Müller, Bartelt, Donner, Villringer, & Brandt, 2003; Nobre, Sebestyen, & Miniussi, 2000). These findings support theories that characterize spatial attention as a "spotlight" or a "zoom lens" (Eriksen & St. James, 1986; Posner, 1980).

Feature-based attention (FBA) directs attention to a non-spatial visual feature, like a particular color, motion, or orientation, and operates independently of and in parallel to spatial attention (Andersen, Muller, & Hillyard, 2009; Hopf, Boelmans, Schoenfeld, Luck, & Heinze, 2004; W. Zhang & Luck, 2009). FBA increases neural activity in the brain region associated with processing of the attended feature (Liu, Larsson, & Carrasco, 2007; Motter, 1994; Muller et al., 2006; Treue & Trujillo, 1999). FBA enhances activity for a selected feature throughout the entirety of the visual field; this global enhancement works independently of the deployment of spatial attention (Andersen, Hillyard, & Muller, 2013; Saenz, Buracas, & Boynton, 2002). FBA appears to spread uniformly across the visual field and modulates sensitivity in areas of the visual field without stimuli (Liu & Mance, 2011; Serences & Boynton, 2007).

While spatial attention and feature-based attention are independent mechanisms, they interact with one another during the early stages of visual processing (Andersen, Fuchs, & Müller, 2011; Leonard, Balestreri, & Luck, 2015). In performing a visual search task, observers may either enhance an attended feature or inhibit distractor features (Treisman & Gelade, 1980; Wolfe, 1994). These enhancements and inhibitions are reflected in electrophysiological responses (Bridwell & Srinivasan, 2012; Forschack, Andersen, & Muller, 2017; Moher, Lakshmanan, Egeth, & Ewen, 2014; Painter, Dux, & Mattingley, 2015; Painter, Dux, Travis, & Mattingley, 2014).

Researchers have studied FBA and its operation across the entire visual field by using EEG to measure steady-state visually-evoked potentials (SSVEPs) (Andersen et al., 2013; Bridwell & Srinivasan, 2012; Forschack et al., 2017; Hasan, Grossman, & Srinivasan, 2017; Muller et al., 2006; Painter et al., 2015, 2014; Störmer & Alvarez, 2014; W. Zhang & Luck, 2009). An area of the visual field that flickers at a constant frequency generates an SSVEP at that frequency in occipital and parietal areas (Norcia, Appelbaum, Ales, Cottereau, & Rossion, 2015). One can observe the effects of attention by measuring the strength of the respective SSVEPs produced by flickering different frequencies at two or more different areas of the visual field. While the typical SSVEP study presents centrally-presented flicker, Painter and colleagues (Painter et al., 2014) took advantage of the global property of FBA by presenting their flicker stimulus in the periphery while having participants perform a visual search task in the fovea. They found that this peripheral display produced SSVEPs when the task in the fovea was demanding and required the use of FBA. In the present study, we follow Painter and colleagues (Painter et al., 2014) by using SSVEP responses evoked by peripheral flicker to track FBA.

A potential application of using peripheral flicker to track attention is to brain-computer interfaces (BCIs). Attention-based BCIs estimate what the user is paying attention to and carry out an appropriate response. While various neural responses have been used by BCIs, the two most common are the P300 response and SSVEPs (Fazel-Rezai et al., 2012; Nicolas-Alonso & Gomez-Gil, 2012; Norcia et al., 2015). In BCIs based on the P300 response, the user is typically asked to attend to a single stimulus within a grid of stimuli, while each stimulus is individually flashed (e.g., P300 spellers (Guger et al., 2009; Krusienski et al., 2010)). The P300 is a positive ongoing deflection in the EEG at about 300ms from stimulus onset, typically elicited by the odd-

ball paradigm, where the signal is stronger when a person attends to a target location and that target location undergoes a change. Single trial classification methods using ERPs have found success using time durations of 125ms and 800ms (Cecotti & Ries, 2017; Nunez, Vandekerckhove, & Srinivasan, 2017). SSVEP-based BCIs present a set of stimuli that flicker at various frequencies; the user selects one of these stimuli to attend. Attention enhances the amplitude of the SSVEP with the frequency that matches that of the attended stimulus (Calore, Gadia, & Marini, 2014; Lalor et al., 2005; Lin et al., 2012; Mun, Cho, Whang, Ju, & Park, 2012). Both on-line and off-line SSVEP-BCIs have found success with trial durations ranging from four to eight seconds per trial (Brunner, Allison, Altstätter, & Neuper, 2011; Ng, Bradley, & Cunnington, 2012; Wan et al., 2016; Won, Hwang, Dähne, Müller, & Lee, 2016; D. Zhang et al., 2010; S. Zhang et al., 2018).

The present study extends that by Painter and colleagues (Painter et al., 2014). We follow them in taking advantage of the global spread of FBA to track the attended feature using flicker presented in the peripheral visual field. In the first experiment, we replicate the finding of Painter and colleagues that SSVEPs evoked by peripheral flicker display can be used to track feature-based attention for subjects wearing a head-mounted display (HMD). In the second experiment, we use the HMD to produce a dynamic virtual environment and test whether FBA can be tracked in this situation. Through our results, we aim to provide a viable way to study the neural mechanisms of FBA in realistic environments and to use these methods in future BCIs.

2.2 Experiment 1

2.2.1 Methods

2.2.1.1 Participants

Twenty participants (mean age 26 years; 8 females) volunteered in the experiment. All participants had normal or corrected-to-normal vision. The study obtained written consent from all participants following protocol HS#2014-1090, which was approved by the University of California, Irvine Institutional Review Board.

2.2.1.2 Stimuli and Apparatus

The experiment was generated using the Unity game engine (Unity Technologies, San Francisco, CA, USA) and was displayed by an Oculus Rift Development Kit 2 head-mounted display (HMD) (Oculus VR, Menlo Park, CA, USA) with a resolution of 1920x1080 (960x1080 pixels

per eye), a refresh rate of 75 Hz, and a field of view of 100º. Visual field angles in the HMD are calculated using the vertical resolution (1080 pixels) and the field of view (100º): 10.8 pixels per visual degree.

Experiment participants performed a conjunction search task (Treisman & Gelade, 1980). Items displayed during the task included blue (1.598 cd/m^2) and green (7.143 cd/m^2) Ts on a black background (0 cd/m^2). Each T was displayed in one of four possible orientations from the upright position: 0º, 90º, 180º, 270º (in clockwise order). An upright T was about 3º high and 2.5º wide. The Ts were placed randomly in a 4x4 array of possible locations that spanned the central 22ºx22º of visual field.

The central search array was surrounded by a circular annulus comprising a blue and green checkerboard pattern (see Figure 1). The circular annulus had an outer radius of 44º and an inner radius of 17.5º, respectively. The green- and blue-colored elements of the circular annulus flickered from green to black and from blue to black, respectively. Two flicker frequencies were used: 12.5 Hz and 18.75 Hz. These frequencies were selected from the limited frequencies that the 75 Hz refresh rate of the display could complete steadily without losing frames. Additionally, these frequencies were close to or fell within the beta band, while differing sufficiently from one another to prevent possible overlap. On half of the trials, chosen randomly, the green parts of the peripheral display flickered at 12.5 Hz while the blue parts of the peripheral display flickered at 18.75 Hz. Both the green and blue parts flickered simultaneously at their respective frequencies. These color-frequency combinations were reversed on the other half of the trials: green elements flickered at 18.75 Hz, while blue elements flickered at 12.5 Hz. The peripheral display flickered only during the visual search phase of each trial.

2.2.1.3 Procedure

Participants viewed 128 trials. Each trial had three phases: cue, visual search, and response (see Figure 1). T targets varied in color (blue or green) and orientation (0º, 90º, 180º, 270º). During the

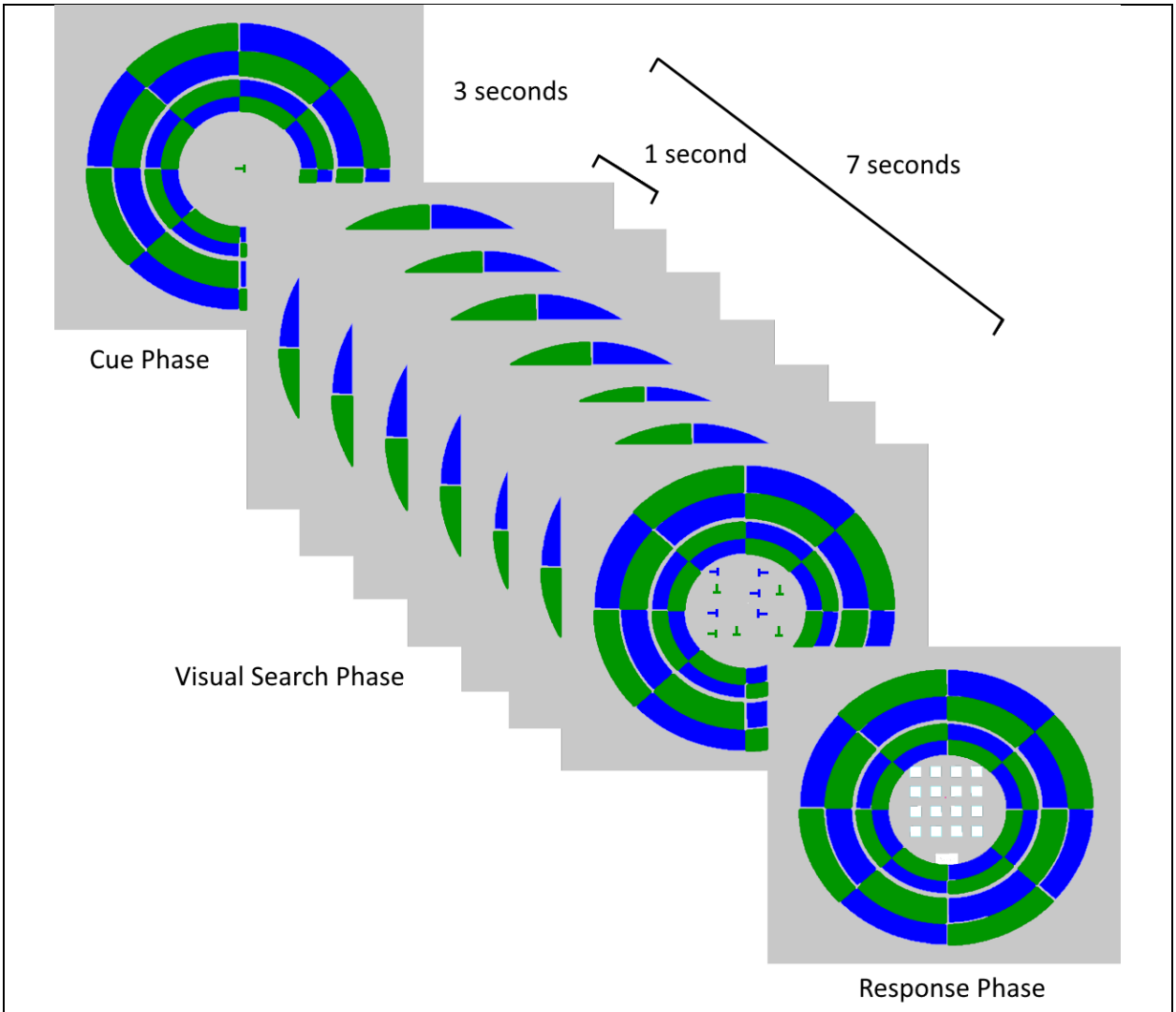

Figure 1. Example progression of a single trial in Experiment 1. First, the cue phase (top left) displays the T-target's color and orientation for at least three seconds. In this example, the T-target is green and oriented 90º. After a button press, the visual search phase begins (middle). This consists of seven sequential search arrays that each have a duration of one second, resulting in a total duration of seven seconds. Each search array has five blue items and five green items that may or may not include the target. The target may appear multiple times within the visual search phase across multiple search arrays, but only once within any individual search array. The subjects' task is to report the location of the last target found. After the seven search arrays have been presented, the subject is shown the response display (bottom right). This shows a 4x4 grid of possible locations. Subjects use the grid to select the location of the last target found. The peripheral flicker display remains in the same location relative to the participant throughout the experiment. It flickers only during the visual search phase. The green and blue components flicker at different frequencies. We used 12.5 Hz and 18.75 Hz as the two flicker frequencies. Color-frequency combinations were counterbalanced across trials. Note that the experiment is displayed entirely by an Oculus Rift DK2 HMD. In consequence, the images shown above do not replicate exactly what subjects see. In particular, the peripheral flicker display lies farther in the periphery than this figure indicates.

cue phase, the T target was displayed for three seconds. The visual search phase was then initiated by a button press.

Following Painter and colleagues (2014), we used a visual search task with known target to direct participants' attention to the target's color. The visual search phase comprised seven different search arrays presented sequentially. Each array lasted one second, so that the full duration of each trial's visual search phase was seven seconds. Each array presented ten items (five blue Ts and five green Ts); each item was a combination of the two possible colors and the four possible orientations. These ten items were randomly placed within a 4x4 array of possible locations. The presented item types and locations changed randomly for each of the seven arrays presented during a single trial.

During a single trial, the target appeared once, multiple times, or not at all. The target appeared at most once within any single search array. The participant responded with the last known location of the target. This task was chosen to ensure that the participant attended to the target color throughout the entirety of the visual search phase. The target had a 10% probability of appearing in the first and second search arrays, a 12.5% chance of appearing in the third and fourth search arrays, a 16.7% chance of appearing in the fifth and sixth search arrays, and a 25% chance of appearing in the seventh search array. The increased probability of a target appearing in later search arrays had the dual purposes of ensuring attention throughout the trial and of decreasing the likelihood of memory interference when multiple targets appeared within a trial. The peripheral display flickered during the entire seven second visual search phase.

The response phase of a trial presented the 4x4 array of possible locations using clear cubes as well as a "None" option. Participants selected the location where they last spotted the target. If the target did not appear during the trial, then they selected the "None" option.

2.2.1.4 EEG Recording and Analysis

EEG signals were recorded using a WaveGuard 64-channel Ag/AgCl electrode cap (which uses the 10/20 system), and an ANT amplifier (ANT Neuro, Enschede, Netherlands). A photocell was used to record flicker on a display monitor that mirrored the HMD. The photocell waveform was used to precisely segment EEG data into trials during offline data analysis. Signals were recorded at a sampling rate of 1024 samples/sec and average referenced offline to the mastoid electrodes. EEG data were recorded continuously throughout the experimental block.

All EEG analyses were conducted offline in MATLAB (The MathWorks, Natick, MA, USA). EEG data were detrended and filtered using a Butterworth bandpass filter that passed energy in the range of 1–50 Hz with 1 dB ripple, and stopbands at 0.25 Hz and 60 Hz with 10 dB attenuation. An additional 60 Hz notch filter was applied to remove power line noise. For each trial, we analyzed data drawn from the start of the third search array to the start of the seventh search array, a total duration of four seconds. These data were designed to be selected prior to analysis following Painter and colleagues to ensure that steady-state responses were analyzed, so excluding data from the first two search arrays and avoiding possible fatigue effects during the final search array (Painter et al., 2014).

For each participant, we examined the steady-state response by first computing the amplitude spectrum for each trial using a Fast Fourier Transform (FFT). We then averaged the amplitude spectra within each condition (Attend Blue at 12.5 Hz, Attend Blue at 18.75 Hz, Attend Green at 12.5 Hz, and Attend Green at 18.75 Hz) to produce condition-averaged amplitude spectra. Finally, we calculated the signal strength for each of the four condition-averaged amplitude spectra for each participant. The signal strength was calculated using methods similar to those of Srinivasan and colleagues (Srinivasan, Bibi, & Nunez, 2006). The signal strength at a target frequency is defined as the ratio of the amplitude at that target frequency to the mean amplitude of the 16 immediately lower and 16 immediately higher frequencies. As we used four seconds of EEG data at a sampling rate of 1024, there was a temporal resolution of 0.25 Hz.

For each condition, we found the six electrodes with the highest participant-averaged signal strength values. Combining electrodes across the four conditions, we found ten total most informative electrodes that produced the highest participant-averaged signal strength across all conditions for Experiment 1. These ten most informative electrodes are: Oz, O1, O2, POz, PO6, PO8, PZ, P8, CPZ, and CZ.

2.2.1.5 Trial Classification Analysis

We tested whether SSVEP responses can be used to predict the color a participant is attending to within a trial. For each participant, we first transformed the EEG data for each trial and each electrode into the frequency domain using an FFT on the observed four seconds. We then calculated the signal strength values, using the same method previously stated, at 12.5 Hz and 18.75 Hz for the 10 most informative electrodes. We used these 20 features (2 frequencies x 10

electrodes) in the trial classification analysis. Each trial was classified into one of two classes, "Attention to color that flickered peripherally at 12.5 Hz" or "Attention to color that flickered peripherally at 18.75 Hz", depending on the flicker frequency of the attended color for the specific trial. We used linear discriminant analysis (LDA), Naïve Bayes (NB) classification, and support vector machine (SVM) as classification methods. LDA and NB classification were executed using the *classify.m* function in MATLAB. SVM classification was executed using code exported from the MATLAB Classification Learner App for the linear SVM classifier. Five-fold cross validation on the 128 trials was used to evaluate each classifier; 102 or 103 trials were used for training and 25 or 26 trials were used for testing for each subject.

Classifier performance was evaluated using measures of: accuracy, area under the curve (AUC), and Matthew's correlation coefficient (MCC).

2.2.2 Results

2.2.2.1 Behavioral Results

In Experiment 1, participants were required to provide the location of the target's last position for each trial. Overall accuracy was found to be 79.18% ± 2.17% (SD = 9.70), which was considerably greater than the chance performance of 6.25%.

We then grouped the data into four conditions with target color (blue, green) and target frequency (12.5 Hz, 18.75 Hz) as factors. A two-way repeated measures ANOVA was used to test whether response accuracy depended on condition (attend blue at 12.5 Hz, attend blue at 18.75 Hz, attend green at 12.5 Hz, and attend green at 18.75 Hz). There was no main effect of color ($F(1,19) = 0.006$, $p = 0.937$) or of frequency ($F(1,19) = 0.603$, $p = 0.447$), and there was no interaction between color and frequency ($F(1,19) = 2.058$, $p = 0.168$).

2.2.2.2 SSVEP Results

SSVEP responses were grouped into four conditions: attend blue at 12.5 Hz, attend blue at 18.75 Hz, attend green at 12.5 Hz, and attend green at 18.75 Hz. We averaged the signal strength values across all participants within each of the four conditions. Figure 2 displays topographic maps of the participant-averaged signal strength for each condition at the attended frequency. These results show that the SSVEP responses appear primarily in the occipital and posterior parietal areas.

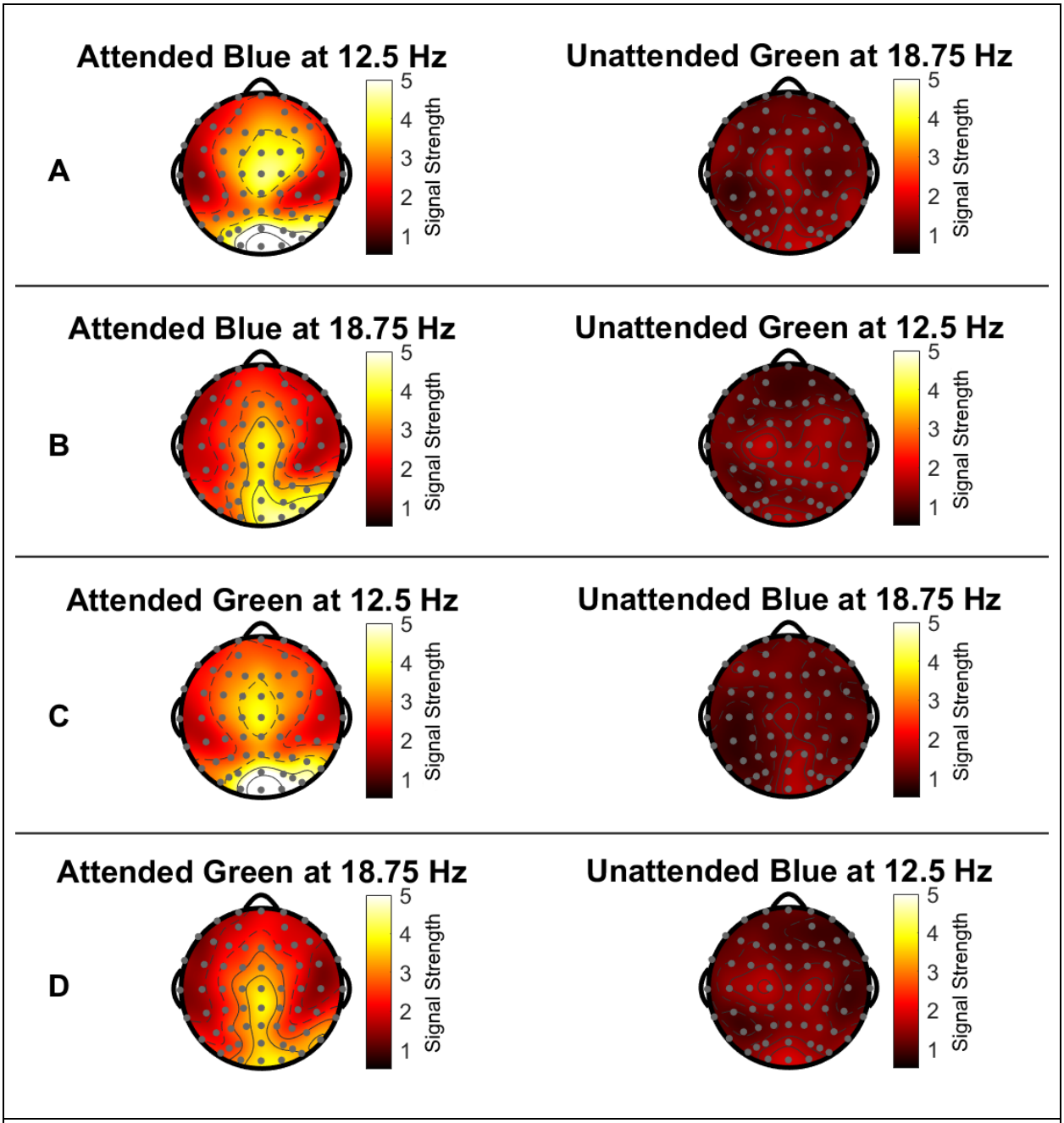

Figure 2. Topographic maps displaying the participant-averaged signal strength at the attended frequency across the scalp for each of the conditions in Experiment 1. The triangle on top indicates the nose and the half ovals on the left and right sides indicate the ears. Dark red indicates low signal strength values and white indicates high signal strength values. Row A are the topographic maps for the Attend Blue at 12.5 Hz condition, displaying the signal strength for 12.5 Hz across the scalp on the left and the signal strength for 18.75 Hz across the scalp on the right. SSVEPs appeared primarily in the occipital and parietal areas. Row B are the topographic maps for the Attend Blue at 18.75 Hz condition, displaying the signal strength for 18.75 Hz across the scalp on the left and the signal strength for 12.5 Hz across the scalp on the left. Again, SSVEPs appeared primarily in the occipital and parietal areas. The figures in Row C and Row D display similar information for the Attend Green conditions.

We assessed the strength of the SSVEPs by averaging the participant-averaged signal strength values across the ten most informative electrodes (see Figure 3). Figure 3 shows the signal strength values for each of the four conditions. In the Attend Blue at 12.5 Hz condition (top left), the attended frequency (12.5 Hz) has a greater signal strength value than the unattended frequency (18.75 Hz). In the Attend Blue at 18.75 Hz condition (top right), the attended frequency (18.75 Hz) has a greater signal strength value than the unattended frequency (12.5 Hz). Equivalent results were found in the respective Attend Green conditions. Throughout each of the four conditions, we observed that the signal strength values for the frequency of the attended color are greater than the signal strength values for the frequency of the unattended color. It should also be noted that there is also a similar response pattern at the second harmonics (i.e. 25 Hz, 37.5 Hz) of both frequencies.

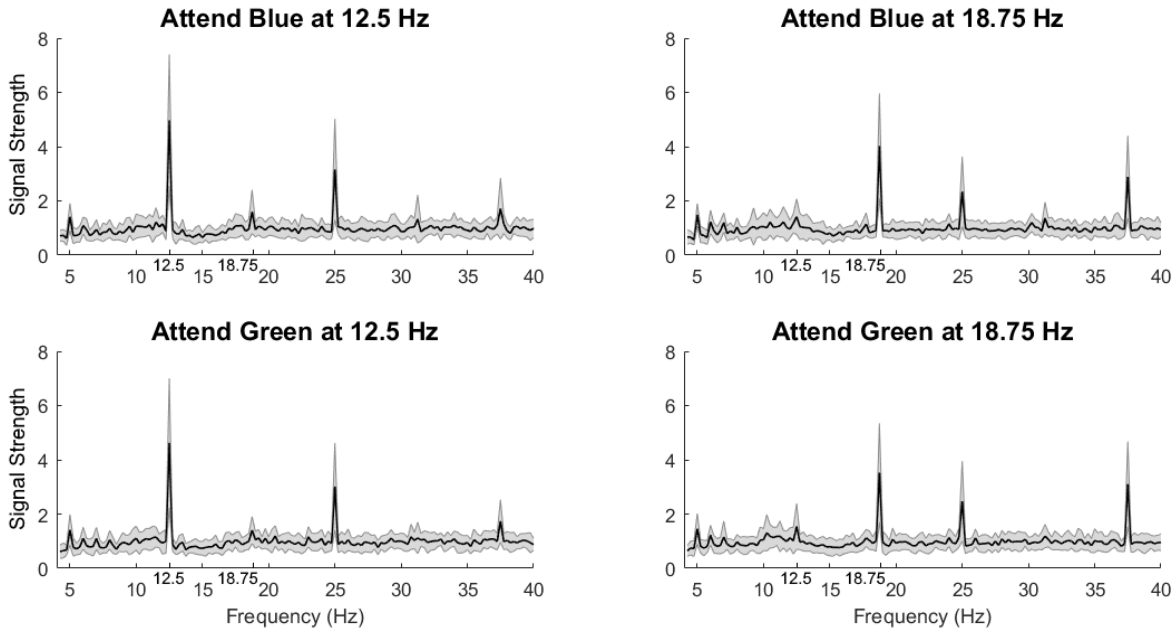

Figure 3. Signal strength as a function of frequency averaged across 20 subjects and the ten most informative electrodes, for each of the conditions in Experiment 1. The horizontal axis displays the frequency values and the vertical axis displays signal strength values. The top-left figure displays the Attend Blue at 12.5 Hz condition, where a high signal strength value at the attended frequency (12.5 Hz) and its harmonic (25 Hz) can be seen as large peaks. The unattended frequency (18.75 Hz) has a much lower signal strength value. Shading represents the standard error of the mean across the 20 subjects. The top-right figure displays the Attend Blue at 18.75 Hz condition, where a high signal strength value at the attended frequency (18.75 Hz) and its harmonic (37.5 Hz) can be seen as large peaks. The unattended frequency (12.5 Hz) has a much lower signal strength value. The bottom figures display information similar to that shown above for the respective Attend Green conditions. In each of the four conditions, SSVEP responses appear for the attended frequencies (12.5 Hz and 18.75 Hz) and their respective harmonics (25 Hz

and 37.5 Hz).

To examine if these responses were significantly different, the signal strength values were submitted to a three-way repeated measures ANOVA with the factors: attention (attended, unattended), color (blue, green), and frequency (12.5 Hz, 18.75 Hz). The effect of attention was significant ($F(1,19) = 50.314$, $p < .000$, $\eta^2 = .726$), with signal strength values greater for attended (M = 4.29, SE = .43) than for unattended (M = 1.49, SE = .10). The effect of color was significant ($F(1,19) = 10.192$, $p < .005$, $\eta^2 = .349$), with signal strength values greater for blue (M = 3.00, SE = .26) than for green (M = 2.78, SE = .23). The effect of frequency was significant ($F(1,19) = 5.931$, $p < .025$, $\eta^2 = .238$), with signal strength values greater for 12.5 Hz (M = 3.15, SE = .29) than for 18.75 Hz (M = 2.63, SE = .23). The interaction between attention and frequency was also significant ($F(1,19) = 5.050$, $p < .037$, $\eta^2 = .210$).

2.2.2.3 Trial Classification Results

We wanted to identify the color an individual was attending to on a given trial using his or her SSVEP response. As described in the methods section, we used LDA, NB, and SVM as our classifiers with a five-fold cross validation. We extracted the classifiers' performance measures by classifying a participant's trial as either "attention to color that flickered peripherally at 12.5 Hz" or "attention to color that flickered peripherally at 18.75 Hz". Table 1 displays the trial classification accuracy results, AUC results, and MCC results for each of the 20 participants in Experiment 1.

Table 1. Trial classification results for each of the 20 subjects (column 1) in Experiment 1 using performance measures of accuracy (column 2), area under the curve (AUC) (column 3), and Matthew's correlation coefficient (MCC) (column 4). Subjects ordered in ascending order from lowest LDA classification accuracy at the top to the highest LDA classification accuracy at the bottom.

Subject	**Accuracy (%)**			**AUC**			**MCC**		
	LDA	NB	SVM	LDA	NB	SVM	LDA	NB	SVM
1	40.71	51.57	48.44	0.36	0.52	0.44	-0.19	0.03	-0.03
2	50.03	54.06	60.16	0.48	0.49	0.59	0.00	0.08	0.20
3	54.52	54.68	62.50	0.56	0.62	0.66	0.09	0.09	0.25
4	57.14	48.40	46.88	0.58	0.53	0.41	0.14	-0.03	-0.06
5	62.49	62.58	54.69	0.64	0.68	0.64	0.25	0.25	0.09
6	63.29	67.11	64.06	0.75	0.76	0.73	0.27	0.35	0.28
7	64.09	63.35	60.16	0.70	0.68	0.68	0.28	0.27	0.20

8	65.60	63.35	67.19	0.71	0.68	0.71	0.31	0.27	0.34
9	68.91	71.88	74.22	0.75	0.77	0.82	0.38	0.44	0.48
10	72.63	67.91	71.88	0.78	0.78	0.79	0.45	0.36	0.44
11	75.69	71.92	78.13	0.83	0.81	0.83	0.52	0.44	0.56
12	76.55	71.20	73.44	0.84	0.78	0.82	0.53	0.42	0.47
13	81.29	75.75	77.34	0.87	0.86	0.85	0.63	0.52	0.55
14	82.12	78.89	77.34	0.89	0.83	0.89	0.64	0.58	0.55
15	85.05	82.03	84.38	0.94	0.89	0.93	0.71	0.65	0.69
16	87.51	82.76	79.69	0.91	0.89	0.88	0.75	0.66	0.59
17	89.14	89.94	89.84	0.96	0.95	0.96	0.78	0.80	0.80
18	91.41	86.77	89.84	0.95	0.93	0.95	0.83	0.73	0.80
19	92.15	85.20	91.41	0.96	0.94	0.97	0.85	0.70	0.83
20	92.18	88.25	90.63	0.97	0.94	0.97	0.84	0.77	0.81
Mean	72.63	70.88	72.11	0.77	0.77	0.78	0.45	0.42	0.44

There were no significant differences between the three classifiers for accuracy ($F(2,57) = 0.08$, $p = 0.92$), AUC ($F(2,57) = 0.02$, $p = 0.98$), and MCC ($F(2,57) = 0.08$, $p = 0.92$). As such, we focused on the LDA classifier for further analyses.

Figure 4 displays the classification accuracies of the 20 subjects organized in ascending order from the lowest LDA classification accuracy to the highest LDA classification accuracy. We had eleven subjects with classification accuracies above 70%, eight subjects with classification accuracies above 80%, and three subjects with classification accuracies above 90%. The LDA's accuracy measure strongly correlated with the other performance measures, AUC ($r = 0.98$, $p < 0.001$) and MCC ($r = 1.0$, $p < 0.001$).

The results show clearly that the SSVEP responses can be used to classify trial condition and, more generally, to track feature-based attention to a particular color. Classification accuracy varies among subjects.

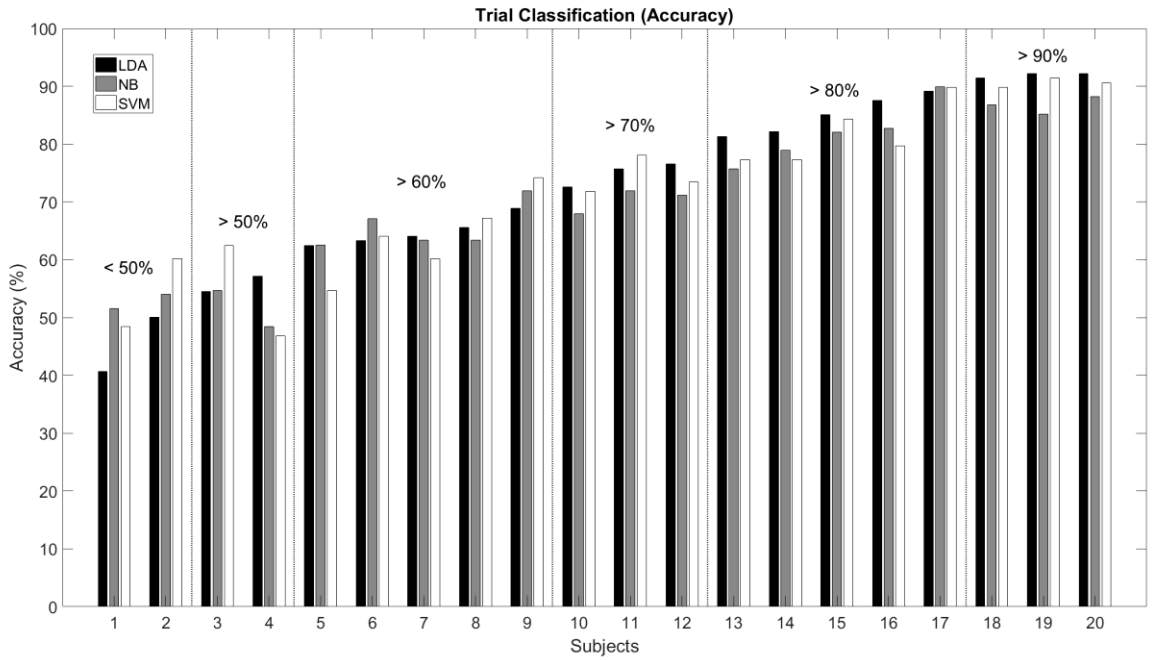

Figure 4. Trial classification accuracy results for each of the 20 subjects in Experiment 1 using the linear discriminant analysis (LDA), Naïve Bayes (NB), and support vector machine (SVM) classification methods. Subjects are organized in ascending order from lowest LDA classification accuracy at left to highest LDA classification accuracy at right. The graph has been segmented into six categories (< 50%, > 50%, > 60%, > 70%, > 80%, and > 90%) based on the LDA classification result. For each subject, LDA accuracies are displayed as black bars, NB accuracies are shown as grey bars, and SVM accuracies are shown as white bars. A 50% accuracy represents chance, as there are two possible classification responses.

2.3 Experiment 2

In the second experiment, we tested whether SSVEPs can be used to track feature-based attention while observers move through a virtual environment.

2.3.1 Methods

2.3.1.1 Participants

Twenty-one participants (mean age 25 years; 10 females) volunteered to participate in the experiment. 17 of the participants in Experiment 1 also participated in Experiment 2. All participants had normal or corrected-to-normal vision.

2.3.1.2 Stimuli and Apparatus

Experiment 2 placed participants in a dynamic virtual environment rather than the static one used in the first experiment. This was achieved by creating a virtual, circular racetrack and placing the observer's camera in a third-person perspective above a virtual car model. For each trial,

participants were moved along the same established path around the racetrack, created using the iTween software (Berkebile, 2010). The racetrack was surrounded by a grey enclosure (see Figure 5). This acted as the background for the search arrays that appeared while participants moved around the racetrack.

2.3.1.3 Procedure

Participants performed a visual search task like that used in Experiment 1. Instead of responding with the last position of the target, participants reported the number of target appearances in each trial. Participants were again presented with 128 trials. These were separated into four blocks of 32 trials with a pause between each block. These breaks between blocks were included to minimize cybersickness. The Simulator Sickness Questionnaire (SSQ) was administered to participants before and after the experiment to help measure cybersickness caused by the experiment (Kennedy, Lane, Berbaum, & Lilienthal, 1993). The SSQ generates a total sickness score which is based on three sub-scores: Nausea, Oculomotor Discomfort, and Disorientation.

Like Experiment 1, each trial in Experiment 2 had three phases: cue, visual search, and response (see Figure 5).

The visual search phase used six search arrays rather than the seven used in Experiment 1. These arrays appeared in sequence as participants moved around the racetrack. Each array's duration was 1.5 seconds, so the full duration of the visual search phase was nine seconds. While Experiment 1 had an increasing probability of a target appearing in later search arrays, Experiment 2 had a constant 25% probability of a target appearing in each of the search arrays.

For the response phase, an input bar was displayed, and participants could use the number pad to enter the number of targets found during the trial (see Figure 5).

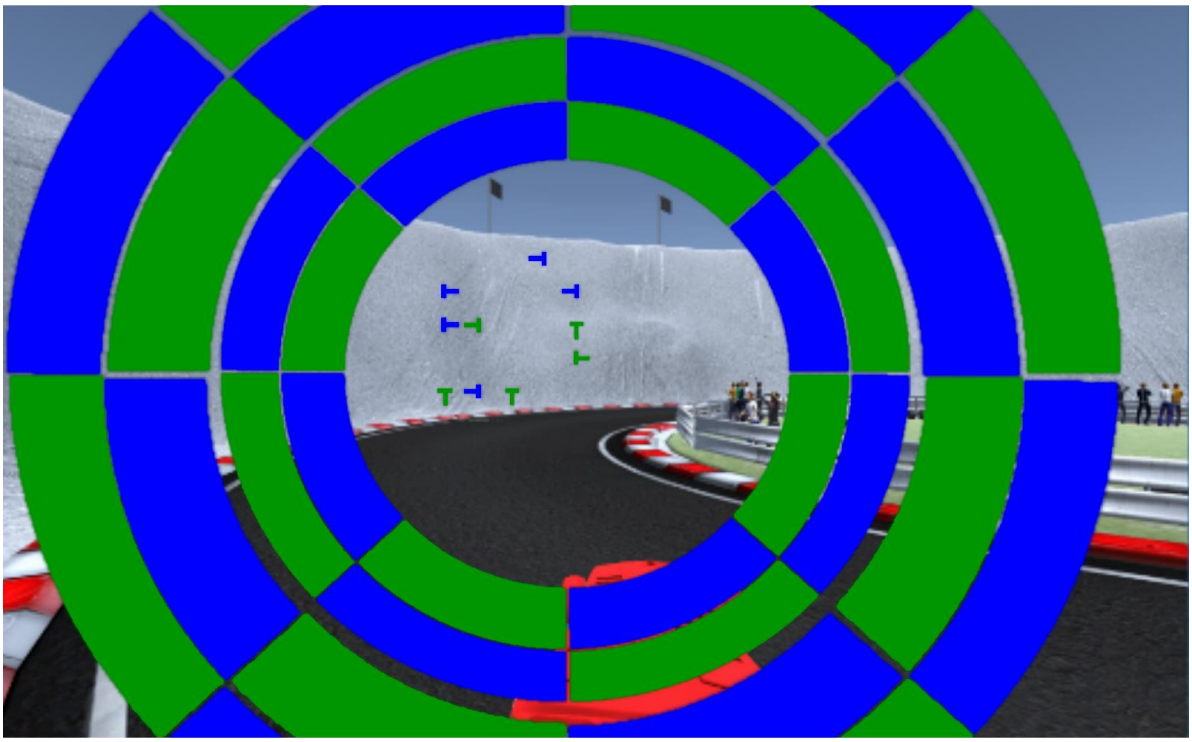

Figure 5. Example image of during visual search phase in Experiment 2. The visual search phase has six sequential search arrays that appeared as participants moved around the racetrack. Each search array has a duration of 1.5 seconds, resulting in a total of nine seconds for the visual search phase. Each search array has five blue and five green items that may or may not include the target. The target may appear multiple times within the visual search phase across multiple search arrays, but only once within any individual search array. Subjects' task is to count the number of targets that appear. The peripheral flicker display remains in the same location relative to the participant throughout the experiment, and flickers only during the visual search phase. The green and blue parts flicker at different frequencies. The green and blue parts flicker at different frequencies, either at 12.5 Hz or 18.75 Hz. Color-frequency combinations were counterbalanced across trials. The experiment is displayed by an Oculus Rift DK2 HMD. In consequence, the images shown above do not duplicate exactly what subjects see. In particular, the peripheral flicker display lies farther in the periphery than this figure indicates.

2.3.1.4 EEG Recording and Analysis

EEG signals were recorded in the same manner as in Experiment 1. As the trials are longer in Experiment 2, EEG data were segmented into nine-second periods corresponding to individual trials. The experiment was designed such that the final second of data from each trial was planned to be removed to avoid possible fatigue and movement artifacts from anticipating the response phase. The remaining eight seconds were used to calculate SSVEP responses using the same methods described in Experiment 1. As there were eight seconds of EEG data at a sampling rate of 1024 Hz, there was a temporal resolution of 0.125 Hz.

We found the six electrodes with the highest participant-averaged signal strength values for each condition. Combining electrodes across the four conditions, we found the ten most informative electrodes that produced the highest participant-averaged signal strength across all conditions for Experiment 2. Across all conditions for Experiment 2: Oz, O1, O2, P2, POz, PZ, CPZ, CP1, CP2, and CZ.

2.3.1.5 Trial Classification Analysis

The classification analysis for Experiment 2 was like that of Experiment 1. The main difference is that four seconds of data per trial were used in Experiment 1, while eight seconds of data per trial were used in Experiment 2.

2.3.2 Results

2.3.2.1 Behavioral Results

Participants responded with the number of targets that appeared within a trial. Overall response accuracy was found to be 73.77% ± 2.41% (SD = 11.02), which is considerably greater than the chance performance level of 14.29%.

We grouped the data into four conditions with target color (blue, green) and target frequency (12.5 Hz, 18.75 Hz) as factors. A two-way repeated measures ANOVA was used to test whether accuracy depended on condition (attend blue at 12.5 Hz, attend blue at 18.75 Hz, attend green at 12.5 Hz, and attend green at 18.75 Hz). There was no main effect of color ($F(1,20) = 1.346$, $p = 0.26$), or of frequency ($F(1,20) = 0.409$, $p = 0.53$), and there was no interaction between color and frequency ($F(1,20) = 0.449$, $p = 0.51$).

2.3.2.2 SSQ Results

The average Total Sickness Score across participants, measured after the experiment, was 10.90 ± 1.98 (SD = 9.08) with a maximum score of 38. The average Total Sickness Score measured before the experiment was only 4.33 ± 1.16 (SD = 5.33); the change suggests that the experiment induced modest motion sickness. For purposes of comparison, the original study that developed the SSQ found a similar mean Total Sickness Score of 9.8 with a maximum score of 108.6 in their simulator sickness study (Kennedy et al., 1993). The current study's sub-scores in Nausea (M = 3.48 ± 0.75, SD = 3.41), Oculomotor Discomfort (M = 4.76 ± 0.69, SD = 3.18), and Disorientation (M = 2.67 ± 0.69, SD = 3.15) were lower than Kennedy and colleagues' sub-

scores in Nausea (M = 7.7, SD = 15.0), Oculomotor Discomfort (M = 10.6, SD = 15.0) and Disorientation (M = 6.4, SD = 15.0). These results suggest that subjects in this experiment suffered somewhat less motion sickness than the average of subjects studied by Kennedy and colleagues.

2.3.2.3 SSVEP Results

Just as in Experiment 1, SSVEP responses were grouped into four conditions: attend blue at 12.5 Hz, attend blue at 18.75 Hz, attend green at 12.5 Hz, and attend green at 18.75 Hz. We averaged the signal strength values across all participants within each of the four conditions. Figure 6 displays topographic maps of the participant-averaged signal strength for each condition at the attended frequency, confirming again that the SSVEP responses appear primarily in the occipital and parietal areas.

The signal strength topographies show that SSVEP responses vary in location with each condition. The most informative electrodes, again, are found primarily over occipital and parietal cortex.

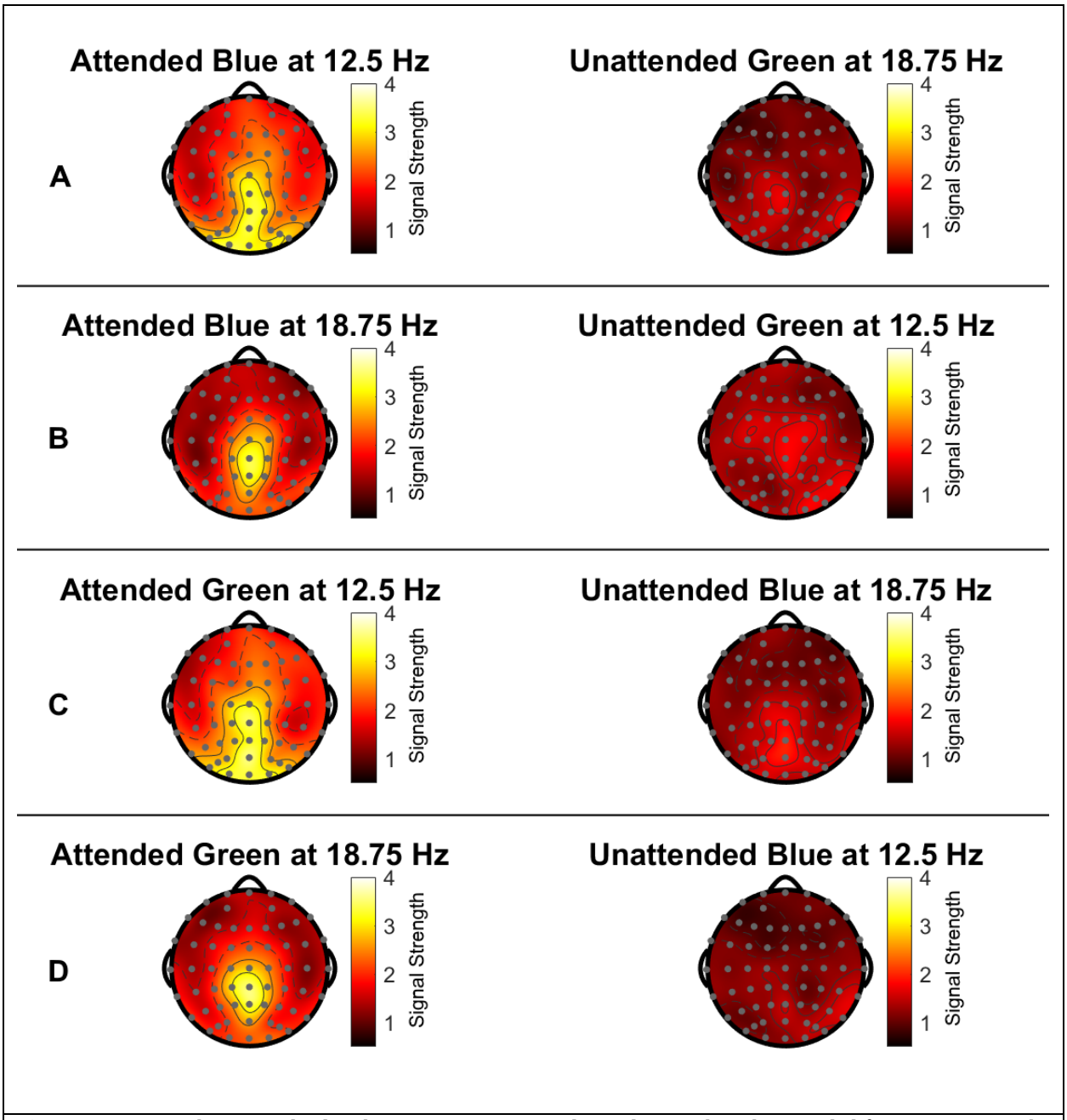

Figure 6. Topographic maps display the participant-averaged signal strength at the attended frequency across the scalp for each of the four conditions in Experiment 2. The triangle on top indicates the nose and the half ovals on the left and right sides indicate the ears. Dark red indicates low signal strength values and white indicates high signal strength values (as per the color bars). Row A are the topographic maps for the Attend Blue at 12.5 Hz condition, displaying the signal strength for 12.5 Hz across the scalp on the left and the signal strength for 18.75 Hz across the scape on the right. SSVEPs appear primarily in the occipital and parietal areas. Row B are the topographic maps for the Attend Blue at 18.75 Hz condition, displaying the signal strength for 18.75 Hz across the scalp on the left and the signal strength for 12.5 Hz across the scalp on the right. Again, SSVEPs primarily appeared in the occipital and parietal areas. The figures in Row C and Row D display similar information for the Attend Green conditions.

We then examined the strength of the SSVEPs in Experiment 2 by averaging the participant-averaged signal strength values across the ten most informative electrodes (see Figure 7). The signal strength values in each condition produced patterns similar to those found in Experiment 1. A greater SSVEP response was generated at the frequency of the attended color, and its harmonics, than at the frequency of the unattended color.

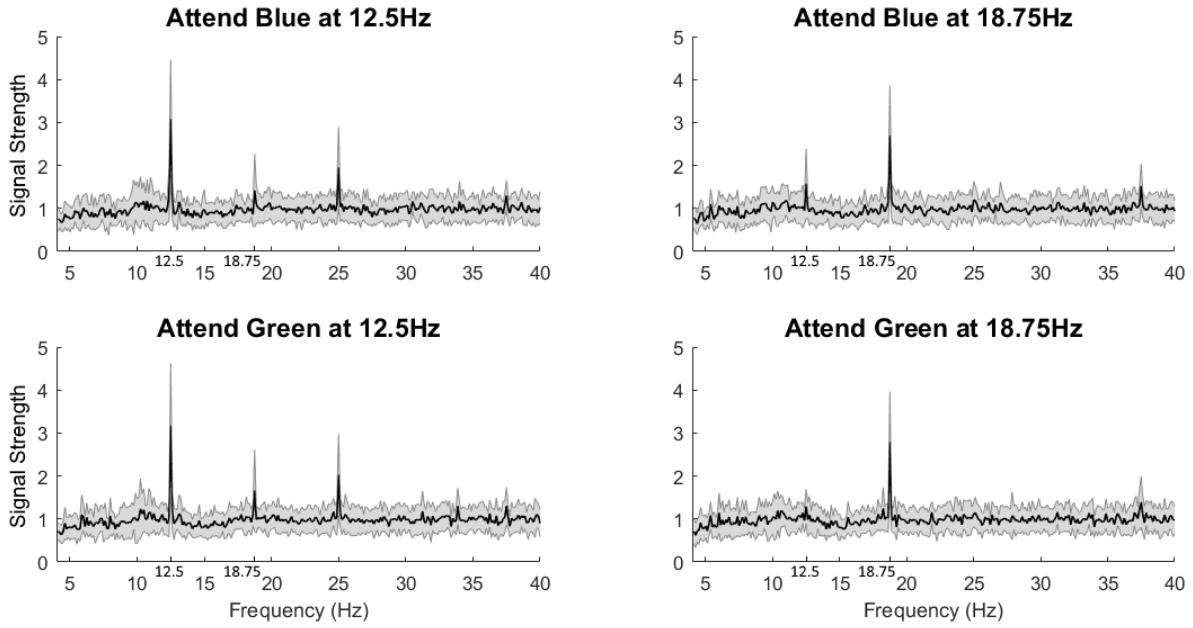

Figure 7. Signal strength as a function of frequency averaged across 21 subjects and the ten most informative electrodes for each of the four conditions in Experiment 2. The horizontal axis displays the frequency values and the vertical axis displays signal strength values. The top-left figure displays the Attend Blue at 12.5 Hz condition, where a high signal strength value at the attended frequency (12.5 Hz) and its harmonic (25 Hz) can be seen as large peaks. The unattended frequency (18.75 Hz) has a much lower signal strength value. Shading represents the standard error of the mean across the 21 subjects. The top-right figure displays the Attend Blue at 18.75 Hz condition, where a high signal strength value at the attended frequency (18.75 Hz) and its harmonic (37.5 Hz) can be seen as large peaks; the unattended frequency (12.5 Hz) has a much lower signal strength value. The bottom figures display similar information as their above counterparts for the respective Attend Green conditions. Throughout the conditions, SSVEP responses appear for the attended frequencies (12.5 Hz and 18.75 Hz) as well as their harmonics (25 Hz and 37.5 Hz), respectively.

To examine if these responses were significantly different, the signal strength values were submitted to a three-way repeated measures ANOVA with the factors: attention (attended, unattended), color (blue, green), and frequency (12.5 Hz, 18.75 Hz). Only the effect of attention

was found to be significant ($F(1,20) = 42.323$, $p < .000$, $\eta^2 = .679$); signal strength values were greater for attended (M = 2.94, SE = .23) compared to unattended (M = 1.49, SE = .11).

2.3.2.4 Trial Classification Results

We used classification methods to see how well SSVEPs can be used to determine the attended color on a given trial. We used the same methods and classifiers (LDA, NB, and SVM) in Experiment 2 as those used in Experiment 1. Table 2 displays the trial classification accuracy results, AUC results, and MCC results for each of the 21 subjects in Experiment 2.

Table 2. Trial classification results for each of the 21 subjects (column 1) in Experiment 2 using performance measures of accuracy (column 2), area under the curve (AUC) (column 3), and Matthew's correlation coefficient (MCC) (column 4). Subjects ordered in ascending order from lowest LDA classification accuracy at the top to the highest LDA classification accuracy at the bottom.

Subject	**Accuracy**			**AUC**			**MCC**		
	LDA	NB	SVM	LDA	NB	SVM	LDA	NB	SVM
1	40.64	58.62	53.13	0.46	0.60	0.57	-0.19	0.17	0.06
2	56.31	60.09	55.47	0.57	0.66	0.61	0.13	0.20	0.11
3	57.78	62.43	60.94	0.65	0.68	0.69	0.16	0.25	0.22
4	58.08	60.18	57.03	0.61	0.67	0.64	0.16	0.20	0.14
5	61.69	68.21	72.66	0.69	0.76	0.76	0.23	0.36	0.45
6	63.29	61.78	65.63	0.65	0.63	0.66	0.27	0.24	0.31
7	63.32	65.71	68.75	0.69	0.71	0.73	0.27	0.31	0.38
8	67.20	64.00	65.63	0.75	0.68	0.74	0.34	0.28	0.31
9	67.97	72.74	74.22	0.77	0.76	0.83	0.36	0.45	0.48
10	71.14	68.74	81.25	0.80	0.79	0.84	0.42	0.38	0.63
11	76.46	76.54	78.13	0.85	0.86	0.85	0.53	0.53	0.56
12	76.62	78.27	77.34	0.83	0.86	0.86	0.53	0.56	0.55
13	78.12	75.77	76.56	0.89	0.81	0.88	0.56	0.52	0.54
14	78.92	72.68	75.78	0.88	0.85	0.87	0.58	0.45	0.52
15	80.34	74.22	78.13	0.84	0.82	0.85	0.61	0.48	0.56
16	80.43	85.17	89.06	0.91	0.93	0.95	0.61	0.71	0.79
17	81.38	82.03	82.81	0.89	0.91	0.91	0.63	0.64	0.66
18	82.00	69.45	81.25	0.88	0.75	0.88	0.64	0.39	0.63
19	88.25	84.34	89.06	0.94	0.92	0.95	0.77	0.69	0.78
20	89.02	86.77	92.19	0.95	0.95	0.96	0.78	0.73	0.85
21	92.12	86.47	87.50	0.95	0.90	0.93	0.85	0.74	0.75
Mean	71.96	72.10	74.40	0.78	0.79	0.81	0.44	0.44	0.49

There were no significant differences between the three classifiers for accuracy ($F(2, 60) = 0.31$,

p = 0.73), AUC (F(2, 60) = 0.25, p = 0.78), and MCC (F(2, 60) = 0.31, p = 0.73). We focus on the LDA classifier for further analyses.

Of the 21 subjects, twelve subjects had classification accuracies above 70%, seven subjects had classification accuracies above 80%, and one subject had classification accuracies above 90% (see Figure 8). The LDA's accuracy measure strongly correlated with the other performance measures, MCC (r = 1.0, p < 0.001) and AUC (r = 0.98, p < 0.001).

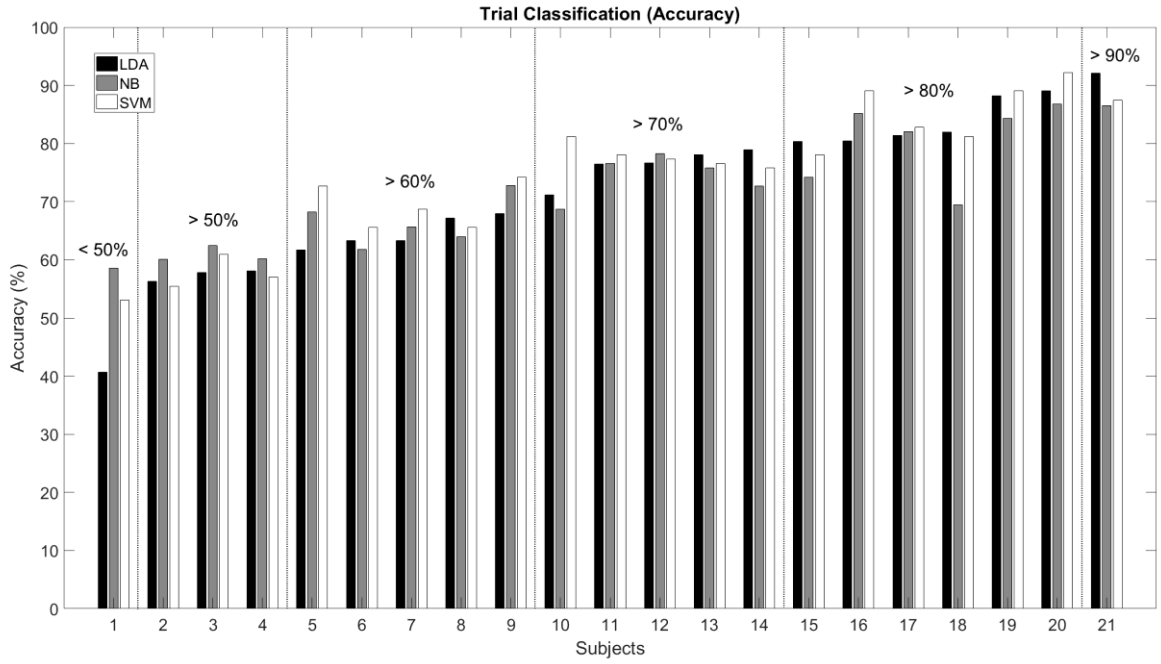

Figure 8. Trial classification accuracy results for each of the 21 subjects in Experiment 2 using the linear discriminant analysis (LDA), Naïve Bayes (NB), and support vector machine (SVM) classification methods. Subjects are organized in ascending order from lowest LDA classification accuracy at left to highest LDA classification accuracy at right. The graph has been segmented into five categories (< 50%, > 50%, > 60%, > 70%, and > 80%) based on the LDA results. For each subject, LDA accuracies are displayed as black bars, NB accuracies are shown as grey bars, and SVM accuracies are shown as white bars. A 50% accuracy represents chance, as there are two possible classification responses.

We then compared the LDA trial classification accuracies for the 17 participants who participated in both experiments (see Figure 9). A paired-samples t-test on accuracies across participants revealed no significant difference in classification accuracies (t(16) = 0.277, p = 0.786) between Experiment 1 (M = 73.13, SD = 16.10) and Experiment 2 (M = 72.25, SD = 13.95). There was also a strong correlation (r = 0.63, p = 0.006) between subjects' Experiment 1

and Experiment 2 accuracies. However, there was no correlation between classification accuracy and behavioral performance for either Experiment 1 or Experiment 2.

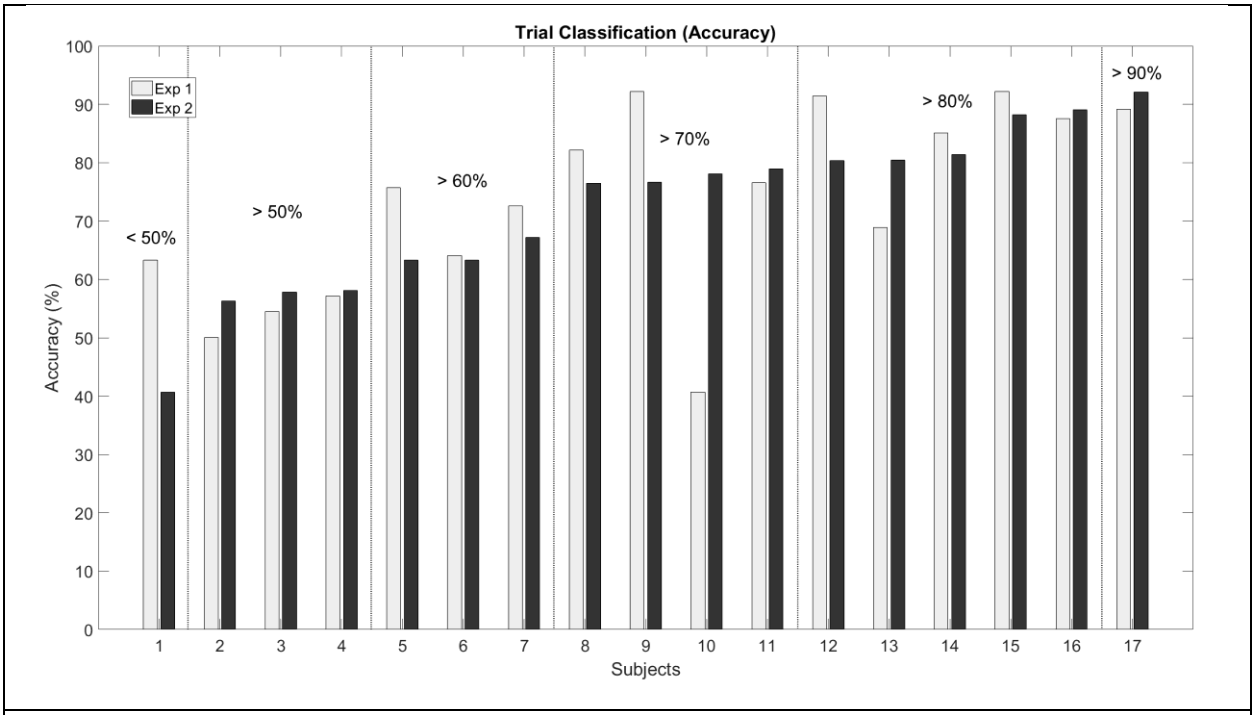

Figure 9. Comparison of LDA trial classification accuracy results for the 17 subjects that participated in both Experiment 1 and Experiment 2. Subjects are organized in ascending order from lowest LDA classification accuracy in Experiment 2 at left to highest LDA classification accuracy in Experiment 2 at right. The graph has been segmented into five categories (< 50%, > 50%, > 60%, > 70%, and > 80%) based on the Experiment 2 results. For each subject, Experiment 1 results are displayed as dark grey bars and Experiment 2 results are displayed as light grey bars.

2.4 Discussion

2.4.1 SSVEP Results

Peripheral flicker displayed in an HMD produces SSVEP responses. SSVEP responses appear in occipital and parietal locations for both of the experiments presented here, a result found earlier by Painter and colleagues (Painter et al., 2014). In both experiments, we consistently found a strong influence of attention on SSVEP responses. We observed a strong response at the frequency of the flickering area with the attended color, and a minimal response at the frequency of the flickering area with the unattended color. This finding is consistent with those found in previous studies of feature-based attention and SSVEP (Andersen et al., 2013; Andersen, Hillyard, & Müller, 2008; Andersen, Muller, & Martinovic, 2012; Bridwell & Srinivasan, 2012).

In Experiment 1, we found significant differences in SSVEPs according to the colors and frequencies used, as well as an interaction of attention and frequency. Painter and colleagues (2014) also found an interaction of attention and frequency in their study. The main effects of color and frequency found in Experiment 1 may be a result of using an HMD. The way that color pixel stimuli are presented in the Pen-Tile matrix AMOLED display used by HMDs is different from the way that these are generated by LED displays used in monitors (Kunić & Šego, 2012; Vauderwange, Curticapean, Dreßler, & Wozniak, 2014). Additionally, the green used had a greater luminance value than the blue used in the experiments. However, the unique artifacts in color production that the HMD's AMOLED display may have introduced in our experiment and the different luminance values between the two colors did not influence the results of Experiment 2. We thus suspect that the effects of color and frequency on the SSVEP responses in Experiment 1 are likely to have arisen because the experiment was stationary and controlled, so emphasizing the presentation differences between the colors and frequencies used. This difference between Experiment 1 and Experiment 2 suggests that, in less controlled and more realistic environments, color and frequency differences become negligible when using an HMD.

SSVEP signal strength values in Experiment 1 were larger than SSVEP signal strength values in Experiment 2. One possible explanation is that the dynamic virtual environment may require increased processing from neural areas other than the ones generating SSVEPs, especially since there are many more sources of distraction compared to the stationary environment (Rousselet, Fabre-Thorpe, & Thorpe, 2002; VanRullen & Thorpe, 2001). Increased activity in other neural areas may result in reduced SSVEP signal strength values. Another consideration is that HMDs are known to induce the side effect of cybersickness in most of its users (Cobb, Nichols, Ramsey, & Wilson, 1999; Dennison, Wisti, & D'Zmura, 2016; McCauley & Sharkey, 1993). Experiment 2 displays optic flow consistent with movement through the virtual environment, despite the subject remaining seated and stationary. Significant but modest cybersickness was produced by Experiment 2. This cybersickness may have impacted visual attention and the size of the SSVEP signal strength. Additional experiments could further explore these underlying effects of stationary and dynamic virtual environments on visual attention.

2.4.2 Trial Classification Results

Trial classification analysis shows that a peripheral flicker display can be used to successfully track feature-based attention in both stationary and dynamic virtual environments. Using the LDA classifier on trials in each Experiment 1 and Experiment 2, we reached classification accuracies averaging 72% across all participants; a significant fraction of subjects reached accuracies above 80%. An examination of classification results for subjects who participated in both experiments found no differences in classification accuracy despite the difference in the two experiments' SSVEP response magnitudes. We conclude that one can use peripheral flicker to track FBA using SSVEPs, whether the observer is in a stationary or a moving virtual environment.

BCI researchers have previously examined possible systems that do not require direct spatial attention. These methods have focused on using covert visual attention, auditory stimuli, and tactile stimuli to control BCIs (Riccio, Mattia, Simione, Olivetti, & Cincotti, 2012). BCI studies examining systems that use visual attention separated from eye movements have so far been limited to forms of covert spatial attention, a form of spatial attention where the user's eyes and attention are not directed at the same location (Tonin, Leeb, & Millán, 2012; Treder, Schmidt, & Blankertz, 2011). One study by Zhang and colleagues (2010) (D. Zhang et al., 2010) explored a design similar to the current study, where objects of two possible colors were presented in the periphery. However, in Zhang and colleagues' study, participants were asked to attend covertly to the peripheral objects rather than to engage in a foveal task. Zhang and colleagues found an average classification accuracy of 71.7%. This suggests that the spatial attention to a peripheral flicker used in Zhang and colleagues and the feature-based attention to a peripheral flicker used in the current study perform similarly. While foveal SSVEP displays may produce stronger and more defined responses, peripheral displays can still be useful in creating flexible and usable BCI systems.

Since we examined the peripheral flicker display as a viable alternative to the foveal flicker display currently used in SSVEPs studies, future work can investigate direct comparisons between the two types of displays to determine tradeoffs between them. These comparisons may examine classification accuracies in offline and online BCI systems and cognitive factors that

may impact user comfort, such as visual fatigue (Cao, Wan, Wong, da Cruz, & Hu, 2014; Mun, Park, Park, & Whang, 2012; Xie et al., 2016).

2.5 Conclusions

The current study explores the use in virtual reality of a peripheral flicker display to produce SSVEPs with the goal of tracking feature-based attention. The first experiment placed observers in a stationary virtual environment and was used to establish that a peripheral flicker display in an HMD generates SSVEPs. The second experiment placed observers in a dynamic virtual environment and used the peripheral flicker display to track observers' feature-based attention to color. Through offline classification, we were able to successfully track an observer's attended color on a trial-by-trial basis. These results show that a peripheral flicker display produces SSVEPs that can be used to track feature-based attention. The use of peripheral flicker lets researchers create more flexible and practical BCIs based on feature-based attention.

2.6 Acknowledgements

Thanks to my advisor and co-author Michael D'Zmura for his various contributions to the project, Mark Dennison for his help with the virtual environment and advice on data analysis, Melissa Morales for her help with data collection, and Andrew Zack Wisti for advice on data analysis. Thanks also to the anonymous Journal of Neural Engineering reviewers for their helpful remarks.

3 Emotion Regulation in the Prisoner's Dilemma: Effects of reappraisal on behavioral measures and cardiovascular measures of challenge and threat

This study was published in *Frontiers in Human Neuroscience* at https://doi.org/10.3389/fnhum.2019.00050

3.1 Introduction

Imagine you are walking along a sidewalk and someone bumps into you and then smiles. You may interpret this smile to be innocuous or malicious. Depending on how you interpret this person's actions and how you regulate your emotions, you may display different behavioral and physiological responses.

Given that it is infeasible to study an individual's responses to someone stepping on his or her foot, we have relied on established paradigms from behavioral economics and cognitive science. The Prisoner's Dilemma is one such experimental paradigm that allows researchers to study social interactions in a controlled environment. In its basic form, the Prisoner's Dilemma is a two-player task where the payoffs for each player depend on the simultaneous choice of both players (Poundstone, 1993). The task creates incentives to cooperate (mutual cooperation yields the largest rewards) but also temptations to exploit the other player, creating a dilemma of trust. The iterated Prisoner's Dilemma allows players to repeat this dilemma over multiple rounds and provides a powerful laboratory to study trust establishment, violation, and repair. The decision to trust is often characterized as an emotional decision and the current study explores how trust repair is shaped by both intrapersonal and interpersonal emotion processes (Dunn & Schweitzer, 2005; Fehr & Gächter, 2002). Specifically, we create a situation where an opponent (a human confederate) initially establishes a lack of trust (by acting non-cooperatively on the first round) and then tries to build trust by cooperating for the remainder of the game). Regarding intrapersonal emotion, people often respond to trust violations with anger and this can undermine their ability to both recognize and accept sincere attempts to repair the relationship. Emotion regulation can help reduce this felt anger and facilitate trust repair. The emotional expressions of the opponent can help intensify or regulate these angry feelings. For example, if opponents smile with genuine pleasure following their betrayal, this can intensify feelings of anger by signaling

the betrayal was intentional and desired (de Melo, Carnevale, Read, & Gratch, 2014). We examine how participant regulation and opponent expressions interact to shape trust repair.

3.1.1 Emotion Regulation and Reappraisal

In the context of social interactions in experimental games, rejection induces anger and motivates costly punishment, leading both players to lose money. By modifying their anger, players might reduce this aggressive tendency and lead them to decide on accepting an attempt at trust repair. The current study focuses on the emotion regulation strategy of reappraisal. Reappraisal involves re-interpreting an emotional stimulus towards a positive direction (Gross, 1999). For example, following a trust violation, a player might distance herself from the situation ("it's just a game") or reinterpret the motives of the other player ("maybe she made a mistake"). Reappraisal is a proactive response to an emotional stimulus that must occur early in the emotion-generative process (Gross, 2002; Gross & John, 2003). This contrasts with other emotion regulation strategies, such as suppression, that focus on downregulating an emotional response after it has fully developed.

Several studies suggest that reappraisal can reduce the tendency towards costly punishment in a variety of economic games such as the Prisoner's Dilemma. For example, Grecucci and colleagues (2013a) taught their participants how to reappraise negative events and reduced the tendency to reject unfair offers in an ultimatum game. In a similar vein, Fabiansson and Denson (2012) reduced costly punishment in the ultimatum game by helping participants reappraise their opponent's intentions, telling participants that their opponent was in a bad mood and not to take their actions personally. Feinberg and colleagues (2012) demonstrate that reappraisal is effective in reducing disgust reactions towards morally provocative situations, leading to more deliberative moral judgments.

3.1.2 The Biopsychosocial Model of Challenge and Threat

The Prisoner's Dilemma also creates a motivated performance situation, in which the biopsychosocial (BPS) model of challenge and threat provides a well-documented theoretical framework to interpret physiological responses (Blascovich, 2008; Blascovich & Seery, 2007). The BPS model of challenge and threat posits that when an individual is placed in a motivated performance situation, cardiovascular response patterns emerge that indicate the individual's position on a continuum between challenge and threat states, which are differentiated by the

degree of vasoconstriction (higher in threat) and cardiac output. The BPS model states that the challenge state occurs when the available mental resources meets or exceeds the situational demands and the threat state occurs when the available mental resources do not meet the situational demands. For example, researchers have found that individuals tend to exhibit the challenge state when they are experienced in a task, as these individuals do not need to expend mental resources learning the task (Blascovich, Mendes, Hunter, & Salomon, 1999).

The relationship between the challenge/threat psychological states and neurophysiological activity is based upon Dienstbier (1989). When in a motivated performance situation, the body activates the sympathetic-adrenal-medullary (SAM) axis and the hypothalamic-pituitary-adrenal (HPA) axis of the neuroendocrine system. The SAM axis sharply increases bodily activity by releasing epinephrine and norepinephrine. The HPA axis increases bodily activity for a prolonged period by releasing cortisol. In the BPS model, the SAM axis is active in both challenge and threat states, but the HPA axis is only active in the threat state (Blascovich, Mendes, & Seery, 2002). An individual's challenge/threat state can be inferred through a pattern of cardiovascular measures that reflect activations by the SAM and the HPA axes.

There are four cardiovascular responses targeted in the BPS model: heart rate (HR), ventricular contractility (VC), cardiac output (CO), and total peripheral resistance (TPR). VC is the time from the initial left-ventricular valve contraction to the opening of the aortic valve; VC is related to the pre-ejection period (PEP): VC = – (PEPtask – PEPbaseline). Cardiac output is the amount of blood pumped out by the heart in liters per minute. TPR is the total amount of vasoconstriction or vasodilation in the peripheral blood vessels: (CO * 80) ÷ mean arterial pressure.

Task engagement is required for cardiovascular analysis in the BPS model to be valid, which is defined as either an increase in HR or an increase in VC (Seery, 2013). Once task engagement is confirmed, the individual's challenge/threat state can be determined. The challenge state is characterized by decrease in TPR, increase in VC, and increase in CO; the threat state is characterized by increase in TPR, increase in VC, and decrease in CO (Blascovich et al., 2002). In general, the challenge state increases blood flow whereas the threat state decreases blood flow throughout the entire body.

In the BPS model, an individual placed in a motivated performance situation can fall more towards the challenge state or the threat state and several factors may influence where he or she falls along this continuum (Blascovich, Mendes, Hunter, Lickel, & Kowai-Bell, 2001; Mendes, Blascovich, Lickel, & Hunter, 2002). In social situations with in-group members, the BPS model has found that the challenge state arises when individuals are socially accepted, and the threat state arises when individuals are socially rejected (Mendes, Major, McCoy, & Blascovich, 2008). The threat state can also arise with uncertainty, as individuals attempt to make sense of an unclear reaction or situation (Khooshabeh et al., 2013). In decision-making situations, loss framing has been found to evoke the challenge state (Khooshabeh et al., 2016). In the current study, we expect players without the reappraisal strategy to exhibit the threat state (greater task demands) when reacting to their opponent's non-cooperation, as they deal with both their emotional reactions and producing a strategy for the game. However, with the influence of reappraisal, we expect players to exhibit the challenge state, as they reduce their emotional reactions and focus only on strategizing for the game.

3.1.3 Effect of Facial Expression

As the Prisoner's Dilemma is a dynamic social situation between two players, we explore how an opponent's emotional expressions may affect players. Facial expressions are important social cues that signal players to their opponent's intentions, which can help players predict cooperation in the Prisoner's Dilemma. Positive expressions, such as smiling, from opponents have led to increased cooperation from the player observing the expression (Reed, Zeglen, & Schmidt, 2012).

Facial expressions are complex, and several possible smiles can be used (Ekman, Friese, & Davidson, 1988). The current study uses a form of the Duchenne smile and the non-Duchenne smile. Duchenne smiles are associated with genuine, positive emotions; they are characterized by both a contraction of the zygomaticus major muscle and a contraction of the orbicularis oculi muscle surrounding the eye. Non-Duchenne smiles are social smiles and are characterized by only a contraction of the zygomaticus major muscle. A previous study found that receiving either the Duchenne smile or the non-Duchenne smile from an opponent has behaviorally produced no differences in cooperation rate in players (Reed et al., 2012). However, it is still unexplored if cardiovascular responses can reveal underlying appraisal differences between receivers of the

two smiles. As the BPS literature offers little information on the influences of facial expressions on challenge and threat states, we investigated the effects of receiving the Duchenne and the non-Duchenne smile during the Prisoner's Dilemma game.

To briefly recap, the current study examines the effects of emotion regulation and interpersonal cues exchanged with opponents on behavioral and cardiovascular measures. First, we hypothesize that subjects instructed with a reappraisal strategy will react to non-cooperation with increased cooperation responses compared to subjects not primed with an emotion regulation strategy. Second, we hypothesize that subjects instructed with the reappraisal strategy will exhibit cardiovascular activity representing the challenge state and control subjects will exhibit cardiovascular activity representing the threat state. Third, we conducted an exploratory analysis comparing a form of the Duchenne smile and a form of the non-Duchenne smile to examine their effects on cooperation responses and cardiovascular activity.

3.2 Method

3.2.1 Participants

Eighty-six paid participants (mean age 40 years; 37 females) recruited through Craigslist participated in the study. The study obtained informed consent from all subjects in accordance with the Declaration of Helsinki. The study was carried out in accordance to protocol UP-14-00321, approved by the University of Southern California Institutional Review Board.

3.2.2 Experimental Procedure

Participants played a version of the iterated Prisoner's Dilemma called the Split-Steal game (see Stratou, Hoegen, Lucas, & Gratch, 2015). As in the Prisoner's Dilemma, the Split-Steal game provides the two players with two options: the cooperative choice or the non-cooperative choice. The cooperative choice leads to the highest payout if selected by both players; however, this choice also places a player at risk for exploitation. If one player selects the cooperative choice and the other selects the non-cooperative choice, then the defector receives a large payoff and the cooperator receives a small payoff. If both players defect, they both receive a small payout. The current study used the same payoff matrix as Stratou and colleagues (2015). The Split-Steal game is a simple extension of the standard game, where the two players play ten rounds with each other.

Prior to the game, the participant was introduced to a female confederate (under the guise of another participant) that would be his or her opponent in the game. Both the participant and the confederate were seated in the same room but were quarantined to individual computer stations. Baseline cardiovascular data was setup for both the participant and the confederate, but cardiovascular data was recorded only from the subject. We recorded five minutes of baseline cardiovascular activity.

Participants were randomly assigned to either the emotion regulation (reappraisal) condition or the no regulation (control) condition. Based on Grecucci and colleagues (2013b), those in the regulation condition were instructed about the reappraisal strategy, and an example of how to use it to reinterpret the other person's actions in a less negative way. The reappraisal strategy example related to being cut off while driving on the freeway, and how anger can be reduced by reinterpreting the event from a disrespectful driver to viewing the other cars as mindless machines. Then they were instructed to think of another negative situation to apply the reappraisal strategy. Participants in the control group read instructions for the experiment and were told to interpret a picture of a man.

After reading the emotion regulation or the control prompt, participants were setup to play the Split-Steal game. On the opening screen, the emotion regulation group was told to practice the reappraisal strategy during the game and the control group was told to simply enjoy the game. Cardiovascular recording began at the start of the Split-Steal game. A webcam streamed the players' faces to each other. The stream was only visible to players during the time interval they received the current round's results; this allowed both players to see their opponent's reaction to the results. For all subjects, the confederate defected in the first round, and then cooperated in the remaining nine rounds. For a randomly selected half of the subjects, the confederate was directed to present a "condescending" smile; in the other half of the subjects, the confederate was directed to present a "genuine" smile. Each experimental session took approximately 50 minutes for each participant.

3.2.3 Cardiovascular Recording

Cardiovascular data were recorded using a Biopac MP150 (BIOPAC Systems, Inc.); signals were recorded at a sampling rate of 2000 Hz. Three measures were collected: impedance, electrocardiography (ECG), and blood pressure. Impedance measures were recorded using a pair

of electrodes placed on the left and right sides of the neck and another pair of electrodes placed on the left and right sides of the torso (under the sternum). ECG was recorded using the modified lead II configuration, where an electrode was placed below the right clavicle and another electrode was placed below the left bottom rib. Blood pressure was measured using a blood pressure cuff placed directly over the brachial artery of the subject's non-dominant hand and finger cuffs placed on the first two fingers to calibrate the measure using the radial artery.

3.3 Data Analysis

3.3.1 Behavioral Analysis

Of the eighty-six subjects that participated in the study, six participants who defected (rather than cooperated) in the first round were removed to focus on responses to betrayal (rather than mutual defection). However, it should be noted that the behavioral results are almost identical if they are included. Additionally, three participants were removed from the main analysis as they were missing smile classification data.

3.3.2 Cardiovascular Analysis

An additional six subjects were removed due to errors during cardiovascular data collection and eleven subjects were removed during pre-processing due to bad waveforms. Thus, there were sixty remaining subjects with intact cardiovascular data for analyses.

The Moving Ensemble Average Pipeline (MEAP) software package (Cieslak et al., 2018) was used to remove confounding artifacts and to create 10-second ensemble averages for each target cardiovascular measure. We focused on the 10-second interval immediately after the non-cooperation outcome is revealed to the subject. For each target measure, ensemble averages of the final minute of baseline recording were similarly calculated using MEAP to produce stable baseline measures. Previous BPS studies have only been able to obtain minimal intervals of 60 seconds; however, MEAP allows for shorter intervals ranging from 10 to 30 seconds. The use of 10-second intervals is supported by previous work that suggests challenge and threat cardiovascular activity occur within 8 to 12 second intervals (Cieslak, 2016).

We created cardiovascular reactivity values (i.e. percentage change from the baseline data) for each of the target measures (Seery, Blascovich, Weisbuch, & Vick, 2004). The cardiovascular reactivity values were used to conduct statistical analyses.

3.3.3 Smile Expression Analysis

Upon further inspection of the experimental session video recordings, we believe that the confederate did not consistently present convincing "condescending" or "genuine" smiles, so this factor may not have been a properly controlled between-subject manipulation. This could possibly be due to vague instructions or lack of facial action unit posing experience by the confederate. As such, we decided to conduct an algorithmic classification of smiles to objectively produce separate categories of the presented smiles. We then examined the produced categories of smiles for their distinguishing facial features.

We analyze the confederate's facial recordings with measures of facial movement, head movements, and smile temporal dynamics to confirm that the smiles presented to participants were appropriate for the respective smile conditions. We included head movements and smile temporal dynamics due to research suggesting their significant impact on perceived smile authenticity (Krumhuber, Manstead, & Kappas, 2007). All facial movements and head positions were tracked offline using the OpenFace software package (Baltrušaitis, Robinson, & Morency, 2016). Smile temporal dynamics was manually annotated for the smiles' onset-apex-offset times and calculated using the tool ELAN (Wittenburg, Brugman, Russel, Klassmann, & Sloetjes, 2006).

Facial movement was measured using action units (AUs) from the standardized Facial Action Coding System (FACS) (Ekman, Friesen, & Hager, 2002). Head movement was measured using head position in the up-down direction and pitch rotation. Smile temporal dynamics were measured using the smile onset, offset, and apex duration. We isolated the time segment of the experimentally manipulated smile (i.e. during Round 1 reveal) and averaged each measure across time. Baseline values were calculated by averaging each measure across the full duration of the Split-Steal game. For each measure, we then calculated the change from baseline value used for smile analysis.

Following Ambadar, Cohn, & Reed (2009), we conducted a K-means cluster analysis (K = 2) in JMP Pro v12 (SAS Institute, Cary, NC) using selected AUs, head position measures, and smile temporal dynamics. AUs were selected for analysis if they were significantly correlated to participant cooperation behavior in Rounds 2 and 3: AU 06, AU 10, AU 12, AU 14, and AU 25.

The Duchenne smile is associated with AU 06 and AU 12, while the non-Duchenne smile is associated with only AU 12.

We found clusters analogous to the genuine "polite" smile and the "amused" smile found in Ambadar and colleagues. The only differences in our results from Ambadar and colleagues are: 1) our amused smile cluster has a longer duration than our polite smile cluster, and 2) we did not find any significant difference for maximum offset velocity (i.e. speed of the smile ending) between the two smile clusters. Corresponding with the original smile groups, the "polite" smile cluster consists of 27 "condescending" smiles and 10 "genuine" smiles and the "amused" smile cluster consists of 28 "condescending" smiles and 12 "genuine" smiles. This confirms that the original smile categories were not properly controlled and distinctive in their respective intended features.

While the presented smiles correspond to the Duchenne and non-Duchenne smiles, there are additional features in the two smile types that are not central to the Duchenne and non-Duchenne smiles. We follow Ambadar and colleagues in characterizing our smiles as "amused smile", the cluster including the Duchenne features, and "polite smile", the cluster including the non-Duchenne features.

3.4 Results

3.4.1 The Effect of Emotion Regulation and Opponent's Smile

3.4.1.1 Behavioral Results

For the behavioral analyses, the 77 participants analyzed were placed in four conditions: control and polite smile (N = 18), control and amused smile (N = 19), regulation and polite smile (N = 19) and regulation and amused smile (N = 21).

We examined the participant's choice to cooperate or defect on the subsequent round (Round 2) across the four conditions. Taking both regulation and opponent's smile into consideration, the choice to cooperate or not on the next round was compared between these four groups in a log-linear analysis. As Pearson's chi-square test cannot accommodate more than one predictor, the log-linear analysis is a generalized linear model that allows for comparison of more than two categorical variables, e.g., polite/amused smile and regulation/control.

This analysis did not find a significant interaction between regulation and smile ($G2 = 6.72$, $p = 0.15$). In the regulation condition, there was no effect ($\chi2 = 0.31$, ns); 15 out of 19 participants who saw the polite smile (78.9%) cooperated and 15 out of 21 participants who saw the amused smile (71.4%) cooperated. The effect of smile only appears in the control condition ($\chi2 = 5.81$, $p = 0.02$), where 16 out of 18 in the control group who saw the polite smile (88.9%) cooperated but only 10 out of 19 participants who saw the amused smile (52.6%) cooperated. Due to the high G2 value, we conducted further analysis examining the cooperation behavior in the emotion regulation and the smile conditions separately. The choice to cooperate or defect on the next round was compared between control ($N = 37$) and regulation ($N = 40$) groups in a chi-square test. There was no effect of regulation on cooperation ($\chi2 = 0.22$, ns); 26 control participants (70.3%) chose to cooperate, and similarly, 30 regulation participants (75.0%) chose to cooperate. These results do not support our hypothesis. The chi-square test comparing polite smile ($N = 37$) and amused smile ($N = 40$) groups on the choice to cooperate or defect on the next round revealed a significant effect ($\chi2 = 4.39$, $p = 0.04$), such that 83.7% of participants who saw the polite smile cooperated on the next round and only 62.5% of participants who saw the amused smile cooperated.

To consider whether the effect might emerge or change over the following round, we also analyzed cooperation rates in Round 3. A log-linear analysis reveals a significant interaction between regulation and smile conditions ($G2 = 12.24$, $p = 0.02$). Specifically, the effect of smile only appears in the control condition ($\chi2 = 6.06$, $p = 0.01$), where 66.7% in the control group who saw the polite smile cooperated on the next round and only 26.3% participants who saw the amused smile cooperated. There was a no significant effect of regulation on cooperation ($\chi2 = 3.15$, $p = 0.076$); 18 control participants (46.2%) chose to cooperate, however, 27 regulation participants (65.9%) chose to cooperate. Though, there was again a significant effect for smile ($\chi2 = 8.48$, $p = 0.004$), such that 73.0% of participants who saw the polite smile cooperated and only 40.0% of participants who saw the amused smile cooperated. We also considered the effect of the participant's gender on cooperation behavior; however, the log linear analysis found no significant interaction of gender with either regulation or smile ($G2 = 1.45$, ns).

Overall, the effect of smile persisted throughout the remaining 8 rounds after Round 2; indeed, on average those in the polite smile condition cooperated more in subsequent rounds ($M = 7.68$,

SE = 0.30) than those in the amused smile condition (M = 5.91, SE = 0.29; F (1, 73) = 17.89, p < .001).

3.4.1.2 Cardiovascular Results

For the cardiovascular analyses, the 60 participants analyzed were placed in four conditions: control and polite smile (N = 14), control and amused smile (N = 13), regulation and polite smile (N = 15) and regulation and amused smile (N = 18).

3.4.1.2.1 Task Engagement

We first ensured the presence of task engagement in the cardiovascular data. Task engagement is a prerequisite to the BPS model and is exhibited by either a significant increase in VC and/or a significant increase in HR from baseline (Seery, 2013). If participants are not engaged, then we will be unable to properly examine challenge/threat responses.

In the control condition, a single-sample t-test found that the VC reactivity value was significantly greater than zero, t(31) = 3.78, p = 0.001 (M = 7.34, SD = 10.98). The HR reactivity was also significantly greater than zero, t(31) = 3.28, p = 0.003 (M = 9.36, SD = 16.16). This confirms that those in the control condition experienced task engagement during the reveal of the opponent's non-cooperation.

In the regulation condition (N = 37), a single-sample t-test indicated that the VC reactivity was not significantly greater than zero, t(36) = 0.77, ns (M = 1.35, SD = 10.64). However, the HR reactivity was significantly greater than zero, t(36) = 3.08, p = 0.004 (M = 7.27, SD = 14.38), which confirms that those in the regulation condition experienced task engagement during the reveal of the opponent's non-cooperation.

We found task engagement in the targeted cardiovascular activity (see Figure 10). With the establishment of task engagement, we proceeded with further cardiovascular analyses using the BPS model.

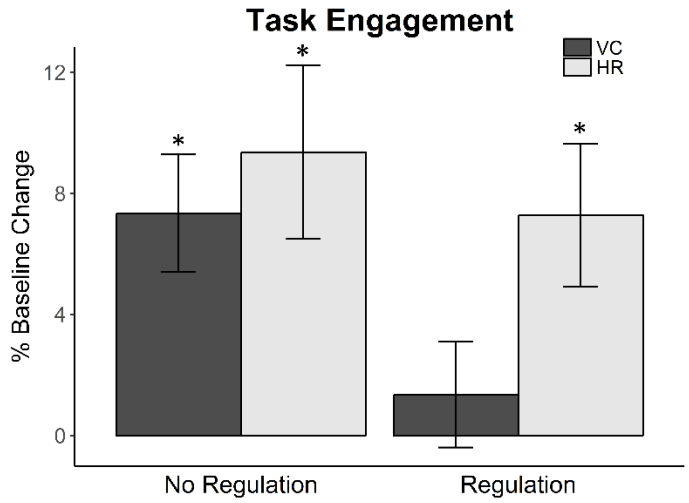

Figure 10. Cardiovascular measures, ventricular contractility (VC) and heart rate (HR), indicate task engagement of participants in both the no regulation control and the regulation conditions. Task engagement is a prerequisite for applying the BPS model of challenge and threat and is determined by increases in either VC or HR. We observed significant increases from zero in both VC and HR for the no regulation control condition, and only a significant increase from zero in HR for the regulation condition; the criteria for task engagement was met for both conditions.

3.4.1.2.2 BPS Model Results

Baseline cardiovascular reactivity measures (TPR, VC, and CO) were compared between these four groups in a two-way MANOVA. This baseline comparison of cardiovascular variables resulted in no significant differences; this ensured that there were no pre-dispositional differences between the two groups.

The cardiovascular reactivity measures (TPR, VC, and CO) were used as dependent variables in a two-way MANOVA consisting of the emotion regulation (control vs. regulation) and smile (polite vs. amused) conditions. This analysis found that the multivariate main effect of emotion regulation (Pillai's Trace = 0.14, $F(3,54) = 2.87$, $p = .05$, $\eta = .14$) was significant with an observed power of .66; however, smile (Pillai's Trace = 0.08, $F(3,54) = 1.49$, ns) and their interaction (Pillai's Trace = 0.03, $F(3,54) = 0.64$, ns) were not significant (see Figure 11). Examining the main effect of emotion regulation, TPR in the control group ($M = -12.04$, $SE = 4.28$) was lower than the regulation group ($M = -2.73$, $SE = 3.89$); VC in the control group ($M = 8.27$, $SE = 2.40$) was higher than the regulation group ($M = 1.11$, $SE = 2.18$); CO in the control group ($M = 12.37$, $SE = 3.61$) was higher than the regulation group ($M = 7.67$, $SE = 3.28$). We

also examined the influence of gender in a three-way MANOVA with emotion regulation, smile, and gender. However, we found that participant's gender (Pillai's Trace = 0.02, F(3,49) = .34, ns) and its interaction with emotion regulation (Pillai's Trace = 0.004, F(3,54) = .50, ns) to be not significant.

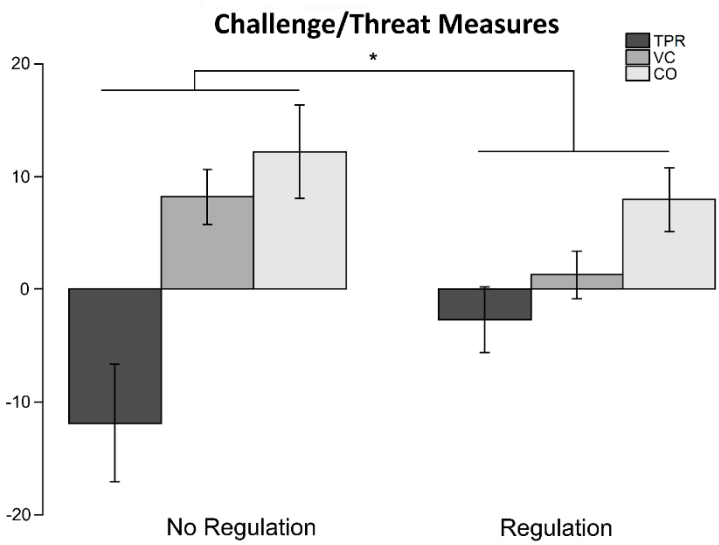

Figure 11. The cardiovascular measures involved in the BPS model of challenge and threat – total peripheral resistance (TPR), ventricular contractility (VC), and cardiac output (CO) – in the control no regulation and regulation conditions. We observed significant differences in a MANOVA of the three cardiovascular measures due to emotion regulation (control vs. regulation). TPR in the no regulation group was lower than the regulation group. VC in the no regulation group was higher than the regulation group. CO in the no regulation group was higher than the regulation group.

Given the multi-variate effect in emotion regulation for our cardiovascular measures, we used a secondary analysis to further examine our effects. We calculated the challenge and threat index, as outlined by Blascovich, Seery, Mugridge, Norris, and Weisbuch (2004), to classify challenge and threat states across all participants. This was done by converting TPR and CO values ($r(69) = -0.80$, $p < .001$) into z-scores, and assigning TPR a weight of -1 and CO a weight of +1; the two values were then summed to create the challenge and threat index. This produces relative challenge and threat differences from the TPR and CO measures. To interpret the challenge and threat index, higher values towards +1 (greater CO compared to TPR) indicate challenge and lower values towards -1 (greater TPR compared to CO) indicate threat.

Given the multivariate main effect of emotion regulation, we focused the challenge-threat index analysis on only the emotion regulation conditions using a Welch's t-test. The t-test did not

reveal any significant differences in index values between emotion regulation ($t(44) = 1.22$, ns) (see Figure 12). A post hoc power analysis using G*Power revealed that to obtain a desired statistical power at 0.80 with $\alpha = 0.05$, we would require 240 subjects for regulation conditions (Faul, Erdfelder, Lang, & Buchner, 2007). This suggests that the transformation to the challenge and threat index score eliminates substantial degrees of freedom and may require a substantial increase in subjects to exhibit the significant difference found in the MANOVA between the emotion regulation conditions.

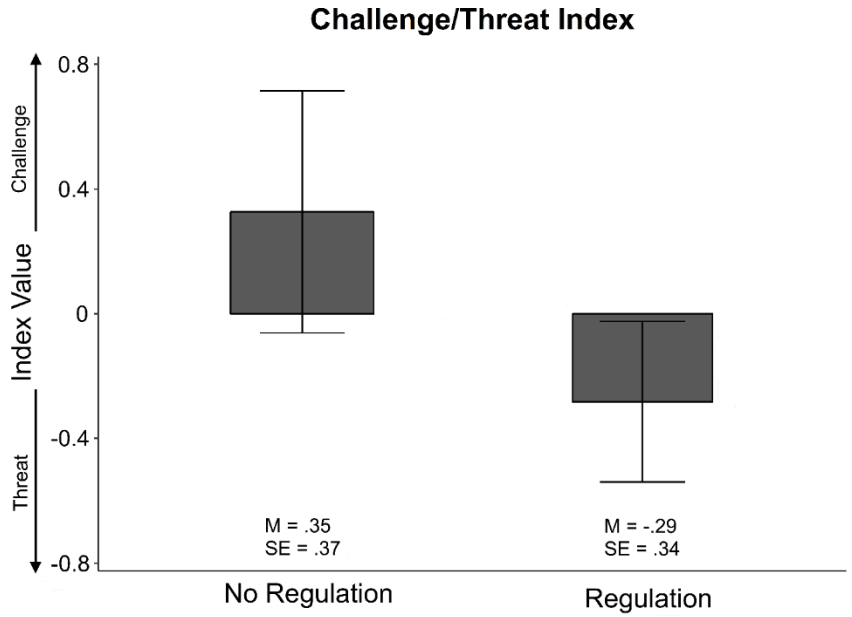

Figure 12. Challenge and threat index values for the control no regulation and the regulation conditions. There were no significant differences between the two index values. However, we note that the no regulation control condition's index value is a higher positive value, aligning closer to the challenge state, and that the regulation condition's index values is a lower negative value, aligning closer to the threat state.

3.5 Discussion

The current study placed participants in a Prisoner's Dilemma scenario, where the opponent defected on the first round. We then explored the effects of reappraisal and the opponent's smile on measures of cooperation behavior and cardiovascular responses.

We predicted that the opponent's smile would not affect cooperation behavior, as previous research found no differences between the amused and the polite smiles (Reed et al., 2012).

Counter to our hypotheses, we found differences in cooperation behavior between the amused smile and the polite smile. Particularly in the control conditions, participants were more likely to cooperate if they saw the polite smile than the amused smile. An explanation for this discrepancy is that Reed and colleagues presented the smiles prior to the decision phase, allowing participants to incorporate the perceived state of their opponent into their decision-making. However, in the current study we present the smiles after the decision is made and participants instead use their opponents' reaction as information for future decisions, changing the context of the smile. Another possible factor is that the current study used a female confederate, which may have influenced perception of smiles across the participants of various demographics. Though, the present dataset did not find any influence of participant's gender on cooperation behavior. Further studies could measure more directly how people perceive the same smiles in different contexts, such as during the decision-making process and after the decision has been made.

We also predicted that the reappraisal group would hesitate to retaliate, manifesting in increased cooperation behavior in the following round (Fabiansson & Denson, 2012; Grecucci, Giorgetta, Bonini, et al., 2013). However, we found no difference in cooperation behavior between the reappraisal group and the control group. Since the present study uses the iterated Prisoner's Dilemma rather than the ultimatum games used in previous studies, the lack of effect by reappraisal may suggest a difference in strategy or other factors specific to the Prisoner's Dilemma. For example, the iterated Prisoner's Dilemma encourages participants to make decisions that have lasting effects, this may lead to the opponent's smile being weighted more than emotion regulation in the decision-making process leading to the observed cooperation behavior.

For the cardiovascular measures, we predicted that the reappraisal group would exhibit activity aligning with the challenge state of the BPS model and the control group would exhibit activity aligning with the threat state of the BPS model. Our initial multivariate analysis indicated that the aggregate cardiovascular measures were different between the reappraisal and the control groups. The control group had lower TPR, greater VC, and greater CO compared to the emotion regulation group. This pattern of cardiovascular measures in the BPS model suggests that the control group experienced the challenge state and, relatively, the emotion regulation group experienced the threat state (Blascovich et al., 2002).

As the results of the multivariate analysis was counter to our hypothesis, this prompted further analysis of the cardiovascular measures using the challenge-threat index measure (Blascovich et al., 2004). The challenge-threat index reflects that the BPS model of challenge and threat is a continuous state that leans toward either challenge or threat rather than a binary state classification. The challenge-threat index yielded no significant differences between the emotion regulation groups; however, a post-hoc power analysis suggests that this measure may not produce enough power to reveal the differences found in the initial analysis. This may be due to the relative nature of the challenge-threat index as it is derived from the absolute TPR and CO measures that were directly used in the initial analysis.

Though the indices between the two groups were not significantly different from one another, the challenge-threat index contains meaningful values in the context of the continuum, as values closer to +1 are associated with the challenge state and values closer to -1 are associated with the threat state. We observed that the relative directions of the challenge-threat index measures between the groups was counter to our original hypothesis and supported the initial results of the multivariate analysis. The resulting challenge-threat indices suggest that reappraisal participants were closer to the threat state, while control participants were closer to the challenge state, albeit statistically non-significant. Future research could examine more directly the relationship of these challenge and threat directionalities with reappraisal and other emotion regulation strategies.

A few factors may have affected the cardiovascular results in the present study. First, the confederate was female, and many of the participants were males; the BPS literature suggests increased threat responses when people interact with out-group members. Though, the present dataset did not find any influence of participant's gender on cardiovascular measures. Second, reappraisal may increase self-awareness of physiological responses, such that reappraisal encourages active monitoring of physiological responses (Jamieson, Mendes, & Nock, 2013; Jamieson, Nock, & Mendes, 2012). If physiological responses are explicitly monitored, then it could lead people to a challenge response as Jamieson and colleagues found. If physiological responses are not explicitly monitored, as in the current experiment, then reappraisal's encouragement for active monitoring may increase mental load and increase the likelihood of a threat response. It seems that the effects of reappraisal on physiological responses may be more

complex than we previously expected. Future studies could compare the effects of various emotion regulation strategies on BPS model of challenge and threat.

In conclusion, the current study examines the effects of reappraisal and an opponent's smile on players who were defected on by their opponent in the Prisoner's Dilemma. In the no regulation control condition, we found that when the opponent expressed an offensive and amused smile, participants were less likely to cooperate the next round than when the opponent expressed a polite smile. In the cardiovascular measures, we found significant differences between the emotion regulation groups. However, further analysis into these differences through the secondary measure of the challenge-threat index found insignificant results. Future work should examine the nature and extent of multi-variable cardiovascular responses during emotion regulation.

3.6 Acknowledgements

Thanks to my co-authors Jonathan Gratch, Peter Khooshabeh, Gale M. Lucas, Su Lei, and Sharon Mozgai for their various contributions to this project. Special thanks to Jonathan Gratch and Peter Khooshabeh for their permission to include this publication in my dissertation. Thanks also to the anonymous Frontiers in Human Neuroscience reviewers for their helpful remarks.

4 SSVEP Measurements of Feature-Based Attention to Color

4.1 Introduction

Several attentional mechanisms facilitate our processing of complex visual scenes when we search for a target item. One mechanism identified in behavioral and electrophysiological studies is spatial attention, where attention to a physical location is enhanced (Eriksen & St. James, 1986; Morgan et al., 1996; N. G. Müller et al., 2003; Nobre et al., 2000; Posner, 1980). Another mechanism is feature-based attention, where attention to a target feature (e.g. color or motion direction) is enhanced independently of physical location (Andersen et al., 2009; Hopf et al., 2004; W. Zhang & Luck, 2009).

Both spatial and feature-based attention perform better when there is greater discriminability between targets and distractors (Duncan & Humphreys, 1989; Nagy & Sanchez, 1990). D'Zmura (1991) suggests that linear detection mechanisms for bottom-up search may enhance target-distractor discriminability. These linear detection mechanisms produce fast search times when target and distractors can be separated by a single line, typically in feature space. When targets and distractors require multiple lines or non-linear functions to fully separate the two stimuli types (i.e. target and distractors are not linearly separable), these linear detection mechanisms are unable to aid search and the difficulty of attentional tasks increases. This effect occurs regardless of the specific features (e.g. color, orientation) and in multi-dimensional feature spaces (e.g. hue and luminance) (Bauer, Jolicoeur, & Cowan, 1996a, 1996b, 1998, 1999; Daoutis, Pilling, & Davies, 2006; Hodsoll & Humphreys, 2001).

Target-distractor discriminability is affected by the distance of distractors in physical space or feature space. Psychophysical and neurophysiological studies exploring the pattern of attentional selection suggest a strong attentional modulation at the target location or feature and a gradual, monotonic decrease in the benefits of attention as the physical distance or feature distance incrementally deviates from the target location or feature (Störmer & Alvarez, 2014; Sun, Chubb, Wright, & Sperling, 2016). Under this model, distractors closer in physical distance or feature similarity to the target increase the difficulty of attentional tasks compared to distractors further away in physical distance or feature similarity (Caputo & Guerra, 1998; Tombu & Tsotsos, 2008). Studies using finer sampling points in distractor distances have further found a surround suppression that appears near the attended location or feature in addition to the

monotonic decrease (Störmer & Alvarez, 2014; Tombu & Tsotsos, 2008; Wang, Miller, & Liu, 2015). This suggests an active suppressive mechanism for distractors with high similarity to the target.

This pattern of attentional selection suggests that there are mechanisms that enhance the response to certain features and others that suppress the response to other features, and these operate simultaneously when one views a scene. Various examples of attentional enhancement and suppression have been examined in electrophysiological studies (Andersen et al., 2013, 2008, 2009; Bridwell & Srinivasan, 2012; Hopf et al., 2004; W. Zhang & Luck, 2009). Researchers have found that feature-based attention enhances target features globally throughout a visual scene. In contrast, feature-based suppression does not seem to be applied globally throughout the visual field; rather, it is a locally applied mechanism that operates when a competing feature is present in the same area as the target feature (Forschack et al., 2017; Hasan et al., 2017; M. M. Müller, Gundlach, Forschack, & Brummerloh, 2018). These global enhancement and local suppression aspects of feature-based attention have allowed researchers to study attention using peripherally flickering stimuli that produce steady-state visually evoked responses (SSVEPs) measured using EEG (Chu & D'Zmura, 2019; Hasan et al., 2017; Jiang, Wu, & Gao, 2017; Painter et al., 2015, 2014).

The current study measures SSVEPs in response to peripheral flicker as the flickering color is systematically varied. This lets us examine the chromatic sensitivity of feature-based attention mechanisms for color. We use SSVEP responses evoked through peripheral flicker to measure the spectral tuning of color detection mechanisms. Our aim is to provide detailed measurements of color detection mechanism sensitivities when we deploy feature-based attention to a particular color is deployed. We also examine how attentional selection is affected by distractor color. We hypothesize that changing distractor colors shifts color-detection mechanisms sensitivities in a way that causes the responses to distractor colors to be suppressed relative to the response to the target color. Colors more similar to a distractor's color will be suppressed, while colors more similar to the target color yet dissimilar to those of the distractors will show an enhanced response.

4.2 Methods

4.2.1 Participants

11 participants (mean age 27.5 years; 7 females) volunteered in the experiment. All participants reported normal or corrected-to-normal vision and normal color vision. All participants provided written consent following protocol HS#2014-1090, which was approved by the University of California, Irvine Institutional Review Board.

4.2.2 Apparatus

The experiment was generated using the Unity game engine (Unity Technologies, San Francisco, CA, USA) and was displayed on a HP LP2475w 24-inch LCD monitor with a 1920 x 1200 resolution and 60 Hz refresh rate. The monitor was calibrated using a spectrophotometer to generate the luminance lookup table that linearized the monitor's luminance (i.e. gamma correction). Participants were placed 60 cm away from the monitor.

4.2.3 Foveal Stimuli

All colors were converted to and manipulated in the DKL color space, which defines a spherical color space that takes into account color-opponent channels in human color vision (Derrington, Krauskopf, & Lennie, 1984). The DKL color space encodes chromatic change using three spherical coordinates: elevation θ (a measure of luminance based on elevation out of the equiluminant plane), chromatic stimulus vector length r (saturation), and azimuth φ (hue).

For each condition, participants adjusted the elevation θ for each of the foveal search task colors (the purple color of the target and the two distractors' colors) so that they appeared equiluminant to the grey background, which was set to 56 cd/m^2, the half-maximum luminance of the display monitor. Participants then adjusted the saturation r of the two distractor colors to match that of the purple target.

During the experiment, participants performed a foveal conjunction search task similar to the one used in Chu and D'Zmura (2019). Throughout the entire experiment, participants sought the same target, an upright purple T (θ = 1.23°, r = 20, φ = 75°), which was shown among distractors of differing color.

The azimuths (hues) of the distractor colors were manipulated across three experimental conditions. They were varied in a way that we hypothesized would influence the sensitivity of

the color filter used to detect the purple target. We measured these sensitivities using SSVEP responses.

There were three conditions (see Figure 13). The neutral condition was presented first for all subjects. The remaining two conditions were counterbalanced across subjects.

The neutral condition used blue-green distractors (φ = 165°, i.e. +90° away from the azimuth of the purple target) and red-orange distractors (φ = -15°, i.e. -90° away from the azimuth of the purple target) with azimuths along the axis in the equiluminant plane that lies orthogonal to that of the purple target.

The blue distractor condition used blue distractors (φ = 120°, i.e. +45° away from the azimuth of the purple target) and yellow distractors (φ = 300°, i.e. +225° away from the azimuth of the purple target and +180° away from the blue distractor color). We hypothesized that using blue distractors would induce participants to use a color detection mechanism that is insensitive to the blue distractors yet sensitive to the purple distractors, namely a detection mechanism biased towards red.

The red distractor condition used red distractors (φ = 30°, i.e. -45° away from the azimuth of the purple target) and green distractors (φ = -150°, i.e. -225° away from the purple target and -180° away from the red distractor color). We hypothesized that using red distractors would induce participants to use a color detection mechanism that is insensitive to the red distractors yet sensitive to the purple distractors, namely a detection mechanism biased towards blue.

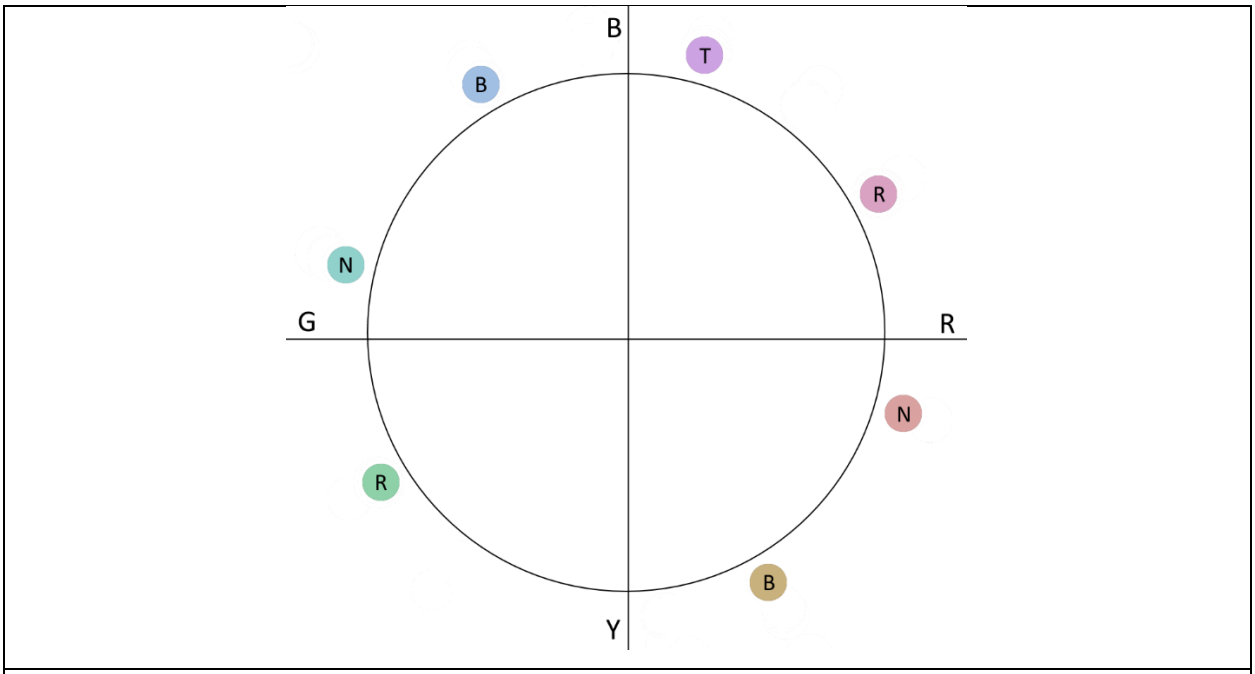

Figure 13. Schematic depiction of the central task's color stimulus hues across the three conditions in the equiluminant plane of DKL color space. The same target is used in all conditions, and is marked by the purple 'T' in the diagram. Neutral condition distractors are marked by 'N', blue condition distractors are marked by 'B', and red condition distractors are marked by 'R'.

4.2.4 Peripheral Stimuli

The peripheral stimulus consisted of an inner and an outer square border surrounding the foveal search task. The two peripheral square borders always had identical colors to one another. The peripheral colors were randomly selected from ten possible colors from trial to trial (see Figure 14). One of the peripheral colors had an azimuth that matched the azimuth of the purple target. Four of the peripheral colors had azimuths that were greater than that of the purple target in steps of 22.5° (+22.5°, +45°, +67.5°, +90°), while a further four had azimuths that decreased in steps of 22.5° (-22.5°, -45°, -67.5°, -90°). The final peripheral color had an azimuth that placed it on the opposite end of the purple target's chromatic axis: 180°. Following Störmer & Alvarez (2014), responses to this color were used as a baseline to determine attentional enhancement or suppression.

The saturation of each peripheral color was adjusted to match the saturation of the purple target. We minimized heterochromatic flicker to adjust the luminance of each peripheral color so that it matched the luminance of the purple target (Lee, Martin, & Valberg, 1988).

During the experiment, the peripheral stimulus was flickered during the foveal search task to produce SSVEP responses. The variation in SSVEP response strength as a function of peripheral stimulus azimuth is a measure of the sensitivity of the chromatic mechanism used to detect the foveal target. The peripheral flicker used a square wave, modulated at 15 Hz, that flickered between the selected peripheral color and black.

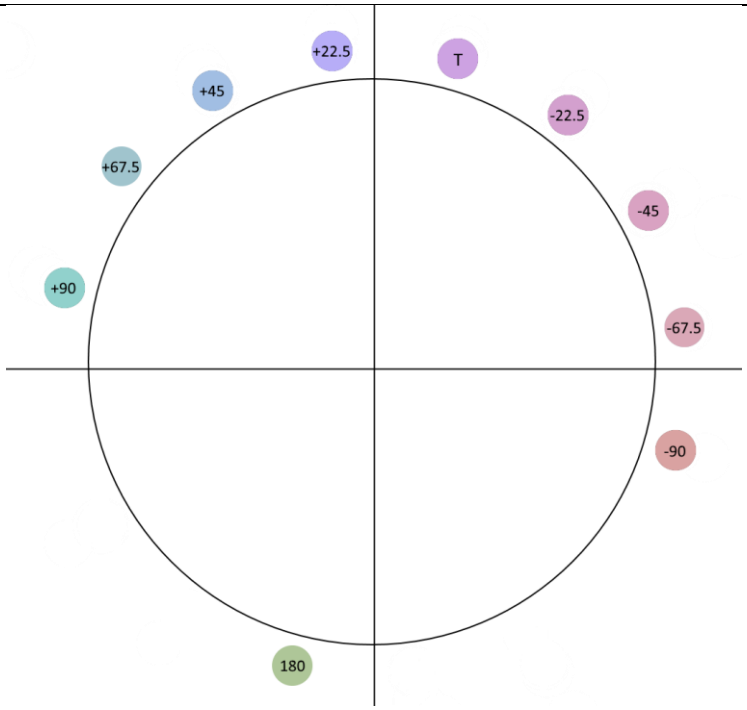

Figure 14. Schematic depiction in the equiluminant plane of the peripheral stimulus hues used in all conditions. The target azimuth is marked by 'T' in the diagram. The numbers indicate the size of the azimuthal angles by which the peripheral stimuli varied in hue from the target.

4.2.5 Procedure

For each of the three conditions, participants completed two blocks of 100 trials of a conjunction search task for a total of 200 trials. In one block, peripheral colors ranged from 0° to +90° away from the target azimuth (hue) across trials, while in the other block they ranged from 0° to -90°. Trials that used the color opposite to that of the purple target, of azimuth 180°, were split between the two blocks. The foveal search task colors remained the same for both blocks of trials.

Each trial had a cue phase, a visual search phase, and a response phase (see Figure 15). During the cue phase, the upright purple T target was displayed for a minimum of one second before

subjects could self-initiate the visual search phase using a button. The visual search phase consisted of four sequentially presented search arrays. Each search array was presented for one second, resulting in a total duration of four seconds for each trial's visual search phase. Each array contained sixteen items: six Ts had the target color, five Ts had one distractor color, and five Ts had the other distractor color. The sixteen items were placed randomly in a 4 x 4 array of possible locations. All of the Ts could be oriented in one of the four possible orientation directions (upright, rotated 90°, upside-down, rotated 270°). The item types and locations changed randomly for each search array.

For each of the two distractor colors' five items, there were luminance and saturation value perturbations made relative to the subject's calibrated stimulus colors: one item had a 5% increased luminance, one item had a 5% decreased luminance, one item had a 5% increased saturation, one item had a 5% decreased saturation, and one item had no change. The perturbed values created a visually detectable change in the items' colors, but not enough to attract bottom-up attentional mechanisms. These perturbations were used to minimize any possible influence of luminance or saturation differences on the search task.

For each individual search array, the trial's target appears only once. However, within the span of the four sequential search arrays, the target may appear in zero, one, two, three, or four of the arrays. The participant is tasked to count the number of times the target appears across the eight search arrays and to enter the final count during the response phase.

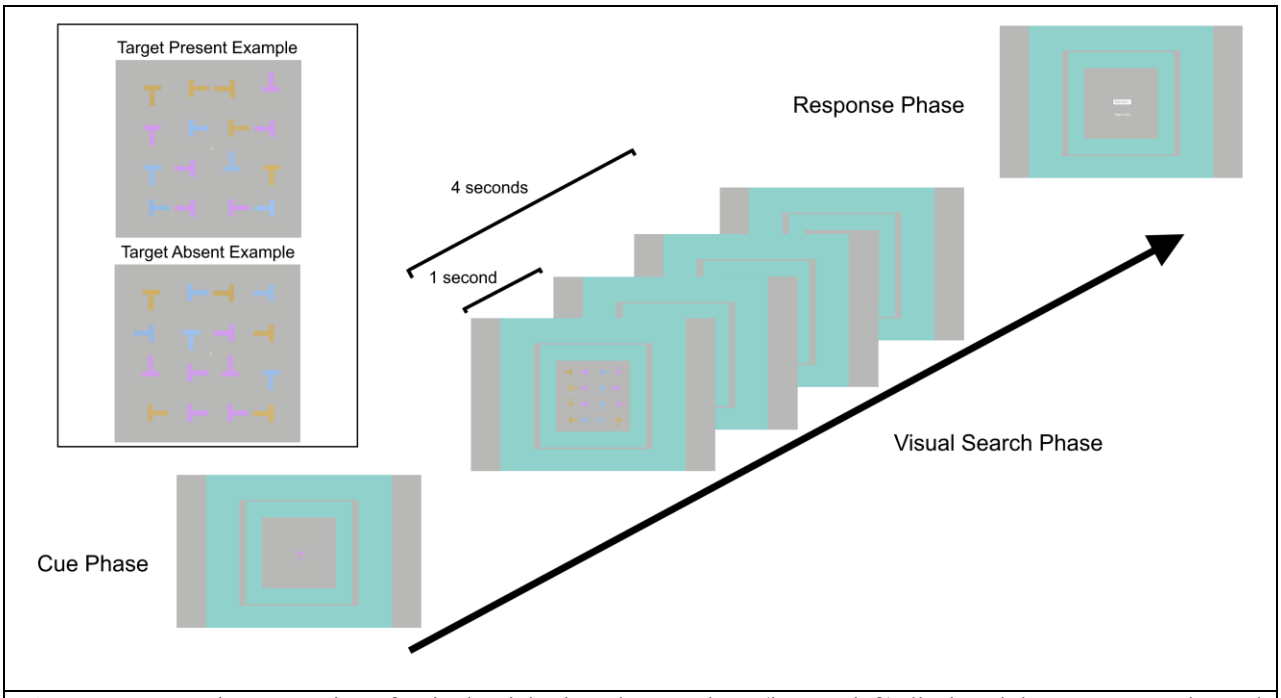

Figure 15. Example progression of a single trial. First, the cue phase (bottom left) displayed the target T's color and orientation – this was the same purple upright-T across all trials and all conditions. After at least a one second delay, subjects could use a button press to initial the visual search phase (middle). The visual search phase consisted of four sequential visual search tasks in a 4x4 array. Each array had a duration of one second, resulting in a total of four seconds for the visual search phase. Each array had six target colored items and five of each distractor item. The purple upright-T target could appear across multiple arrays, but only once within any specific search array. Subjects were tasked with counting the number of times the target appeared within the trial. The final response phase let subjects enter the counted number.

4.2.6 EEG Recording and Analysis

EEG signals were recording using a Cognionics Quick-20 wireless dry EEG headset with 20 electrodes following the 10/20 system (Cognionics Inc., San Diego, CA, USA). Signals were recorded at 1000 samples/sec and recorded using Cognionics Data Acquisition Software Suite (Cognionics Inc., San Diego, CA, USA) and synchronized with stimulus events from the Unity program using LabStreamingLayer (LSL). Impedance values were kept below 200 ohms.

All EEG analyses were conducted offline in MATLAB (The MathWorks, Natick, MA, USA). EEG data were detrended and filtered using a Butterworth bandpass filter set at 1–50 Hz, a 1dB ripple with stopbands at 0.25 Hz and 60Hz, a 10dB attenuation, and a 60 Hz notch filter to remove power line noise. Each trial was segmented using time markers that indicated each trial's onset sent by the Unity program and time matched using LabStreamingLayer to the EEG data.

For the remaining EEG analyses, we analyzed data only from trials where subjects responded with the correct response. We calculated the steady-state response for each participant by computing the amplitude spectrum for each trial using a Fast Fourier Transform (FFT), averaging the amplitude spectrum within each peripheral condition, and finally, calculating the signal-to-noise ratio (SNR). The SNR was calculated using the ratio of the amplitude of the target frequency to the standard deviation of the surrounding 16 frequency bins (8 above target frequency and 8 below target frequency) (Srinivasan et al., 2006). With a sampling rate of 1000 Hz and a total of four seconds for each trial, we had a frequency resolution of 0.25 Hz.

4.3 Results

4.3.1 Behavioral Results

We averaged behavioral accuracy across all subjects and found for the neutral condition an average accuracy of 86.18% ± 3.14% (SD = 10.42), for the blue condition an average accuracy of 90.86% ± 1.70% (SD = 5.63), and for the red condition an average accuracy of 87.45% ± 3.41% (SD = 11.32) (see Figure 16). Note that the neutral condition was always presented first, so that the average performances may be influenced by this order effect. A one-way ANOVA on the accuracies across the three conditions (neutral, blue, and red) found no significant differences between the three conditions ($F(2,30) = 0.72$, $p = 0.495$).

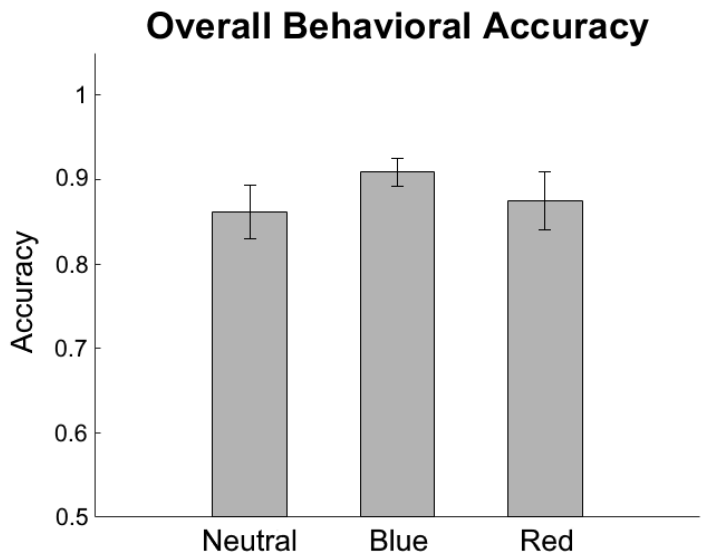

Figure 16. Overall accuracy for all eleven subjects across distractor conditions. The neutral condition, with distractors at ±90° away from the target color, had an average accuracy of 86.18% ± 3.14%. The blue condition, with distractors at +45° and +225° away from the target color, had an average accuracy of 90.86% ± 1.70%. The red condition, with distractors at -45° and -225° away from the target color, had an average accuracy of 87.45% ± 3.41%.

Five subjects consistently performed better than the remaining subjects. This led us to run *post-hoc* analyses comparing the five high-performing subjects, with the highest accuracies across all conditions, to the remaining six subjects to determine whether there were significant differences between subject groups (see Figure 17). The high performers yielded average accuracies of 92.80% ± 2.0% (SD = 4.48) in the neutral condition, 95.40% ± 1.29% (SD = 2.88) in the blue condition, and 95.50% ± 1.35% (SD = 3.02) in the red condition. The low performers yielded average accuracies of 80.67% ± 4.49% (SD = 10.99) in the neutral condition, 87.08% ± 1.78% (SD = 4.35) in the blue condition, and 80.75% ± 4.66% (SD = 11.42) in the red condition.

A two-way ANOVA on the accuracies of the two subject groups (high performers, low performers) and the three conditions (neutral, blue, and red) found only a main effect of subject group ($F(1,27) = 20.97$, $p < 0.001$). There was no main effect of condition ($F(2,27) = 1.05$, $p = 0.365$) and no interaction between subject group and condition ($F(2,27) = 0.51$, $p = 0.604$). Due to this difference in subject group performance, further analyses examine the SSVEP responses

of the two groups of subjects separately in order to determine different strategies in attentional selection.

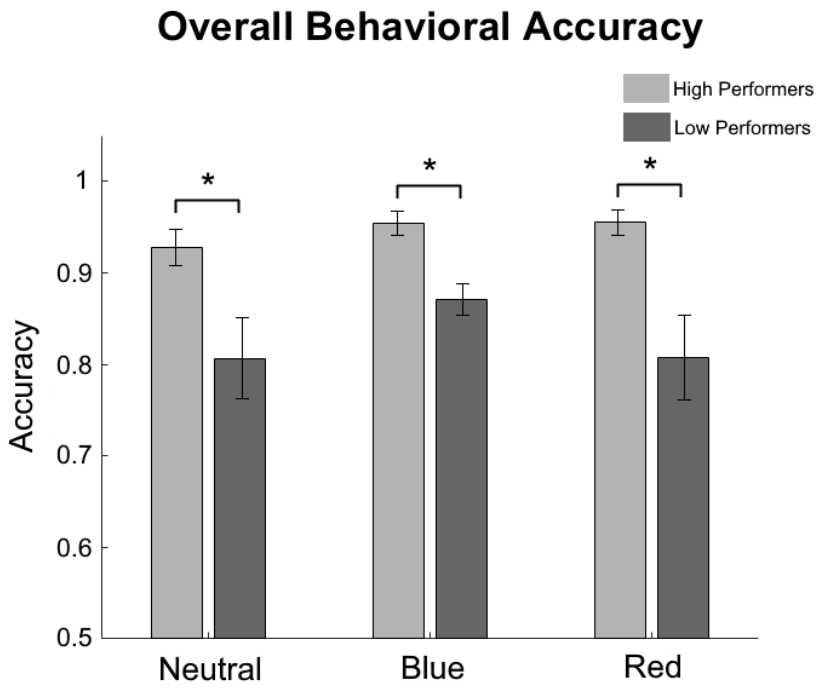

Figure 17. Overall accuracy grouped by high performers (n=5), light grey, and low performers (n=6), dark grey, across distractor conditions. For the neutral condition, distractors at ±90° from the target color, high performers had an average accuracy of 92.80% ± 2.0% and low performers had an average accuracy of 80.67% ± 4.49%. For the blue condition, distractors at +45° and +225° from the target color, high performers had an average accuracy of 95.40% ± 1.29% and low performers had an average accuracy of 87.08% ± 1.78%. For the red condition, distractors at -45° and -225° from the target color, high performers had an average accuracy of 95.50% ± 1.35% and low performers had an average accuracy of 80.75% ± 4.66%.

4.3.2 EEG Results

Figure 19 displays the participant-averaged signal-to-noise ratios (SNRs) in the frequency domain for each peripheral stimulus in the neutral condition. We see the expected peaks at 15 Hz (the flicker frequency) and at its harmonic 30 Hz.

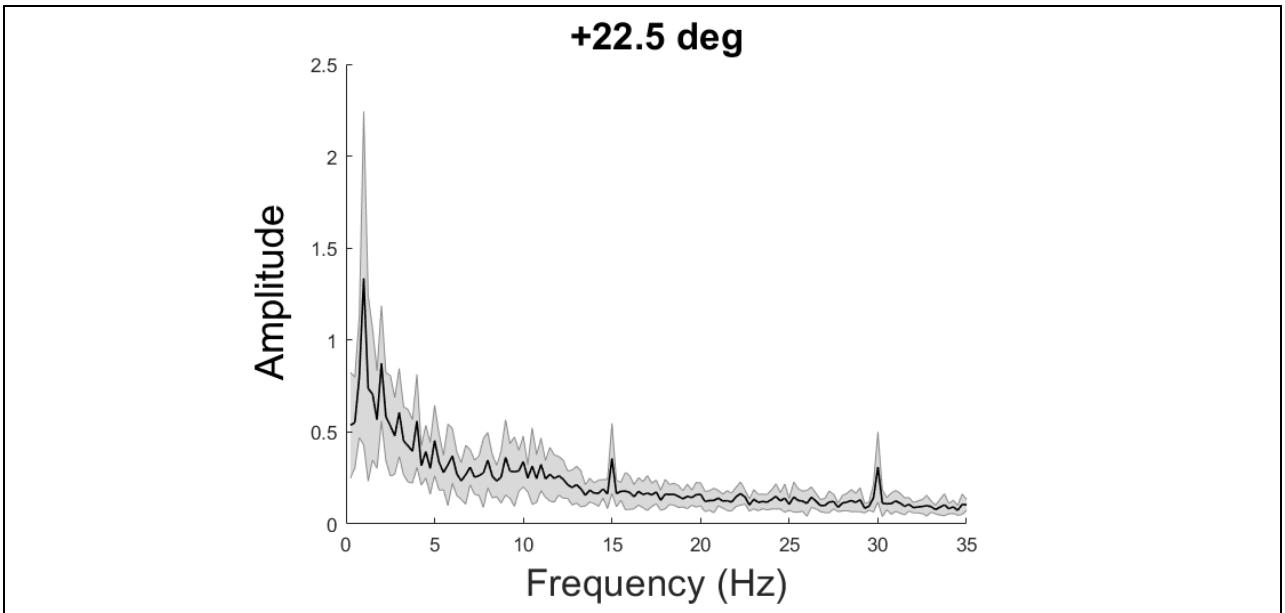

Figure 18. Raw amplitude spectrum plot displaying the target channel-averaged and participant-averaged amplitudes for peripheral at azimuth color +22.5° away from target color in the neutral condition. Peaks for the target frequency (15 Hz) and its second harmonic (30 Hz) in the raw.

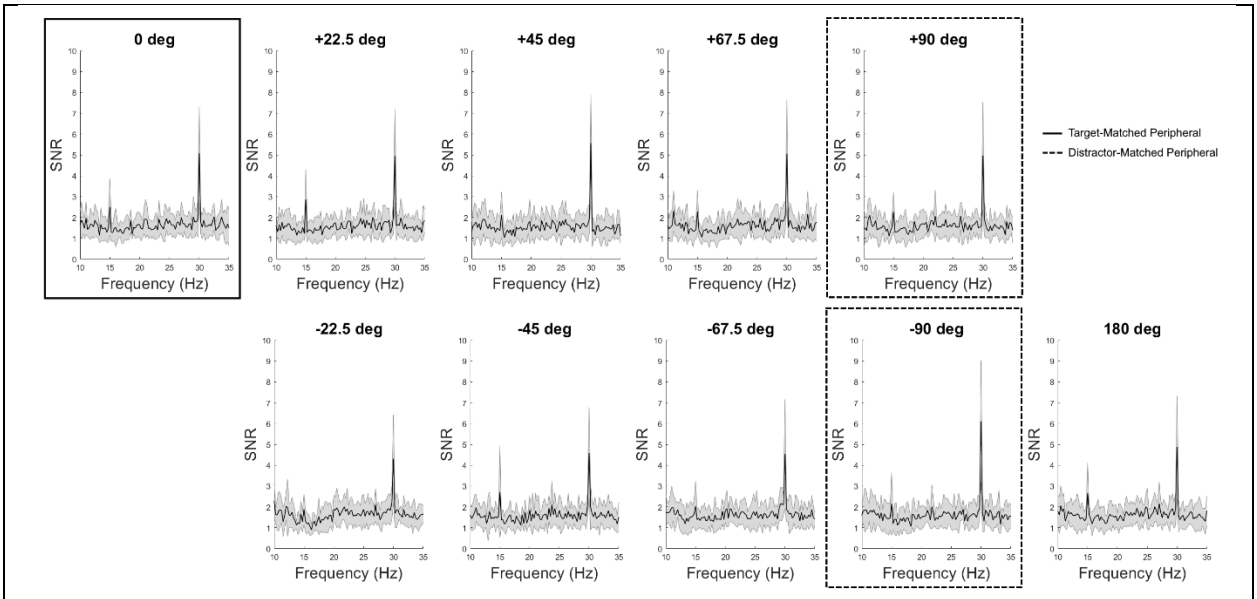

Figure 19. Frequency plots displaying the target channel-averaged and the participant-averaged SNRs for each peripheral stimulus in the neutral condition. Peaks can be seen at the target frequency (15 Hz) and its second harmonic (30 Hz). The solid-lined box highlights the peripheral stimulus that matches the target color. The dashed-lined boxes highlight the peripheral stimuli that matches the two distractor colors in the control condition.

Figure 20 displays topographic maps of the participant-averaged SNR at the 15 Hz flicker frequency for each peripheral stimulus in the neutral condition. The topographic maps for the neutral condition confirm that the SSVEP responses occur in the occipital and posterior parietal areas regardless of the specific peripheral flicker stimuli. For the following analyses, we normalized the electrode responses across each condition using z-scores, averaged the normalized values across conditions, and used the resulting values to create electrode weights.

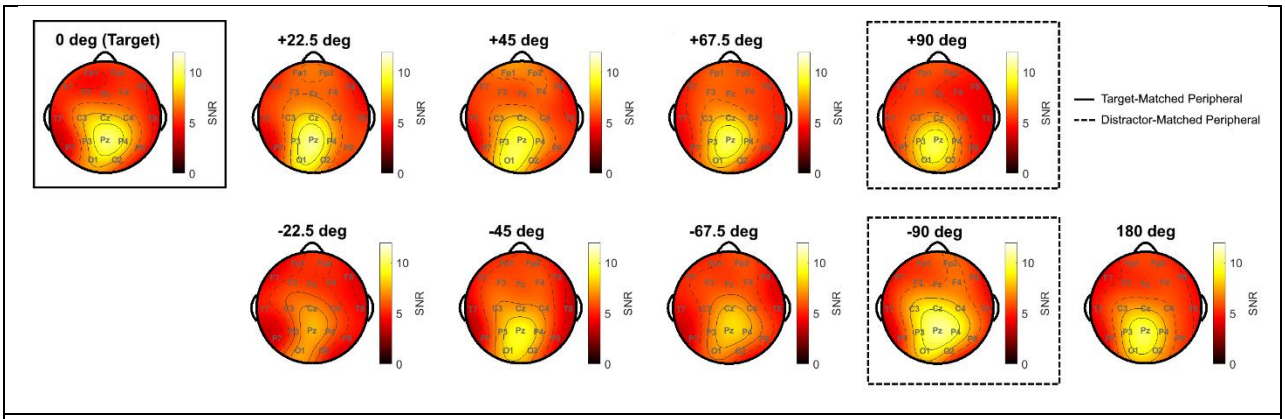

Figure 20. Topographic maps displaying the participant-averaged SNR at the target frequency (15 Hz) and its second harmonic (30 Hz) for each peripheral stimulus in the neutral condition. The solid-lined box highlights the peripheral stimulus that matches the target color. The dashed-lined boxes highlight the peripheral stimuli that match the two distractor colors in the control condition.

Figure 21 displays the SNR values at the flicker frequency for each peripheral stimulus in each condition, averaged within each of the two subject groups: low performers in the top row and high performers in the bottom row. The high performers have generally higher SNR values. In the neutral condition, the high performers exhibited a pattern, where the peripheral stimulus with the color of the attended target had an increased peak, and the surrounding peripheral colors are decreased. On the other hand, the low performers seem to be biased, such that the positively deviating peripherals (towards blue) had higher SNR values.

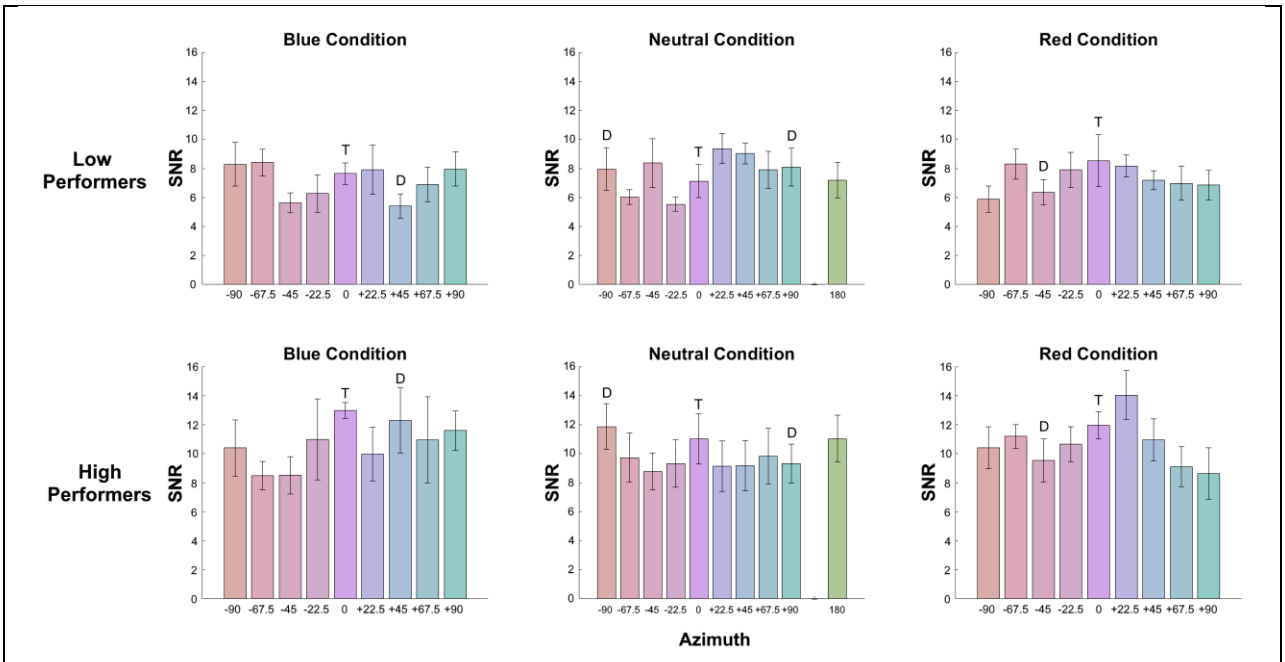

Figure 21. Bar plots displaying channel-averaged and participant-averaged SNRs for all subjects at the target frequency for each peripheral stimulus in each of the three conditions (neutral, blue, and red). The top row displays the results for the low performers and the bottom row displays the results for the high performers.

I will first describe the results of ANOVAs using the data presented in Figure 21. Then I will transform the results (Figure 22) in a way that makes the effects of color condition on detection mechanism sensitivity more apparent. To compare the two groups and the peripheral colors of interest, we ran mixed ANOVAs for each condition on the SNRs comparing the peripheral colors of interest (target and the condition's distractors) between subject groups.

For the neutral condition, there was a significant difference between the subject groups ($F(1,9) = 5.533$, $p = .043$, $\eta^2 = .381$). There was no significant main effect for the peripheral colors of interest (target and two distractor) ($F(2,8) = .421$, $p = 0.670$) and no interaction effect between the peripherals of interest and subject group ($F(2,8) = .469$, $p = .642$) for the neutral condition. *Post-hoc* independent-sample t-tests between the two subject groups did not find any significant differences for target color ($t(9) = 1.953$, $p = .083$), distractor color -90 deg ($t(9) = 1.812$, $p = .103$), or distractor color +90 deg ($t(9) = .653$, $p = .530$).

For the blue condition, there was a significant difference between subject groups ($F(1,9) = 21.476$, $p = .001$, $\eta^2 = .705$). There was no main effect for the peripheral colors of interest (target and blue distractor) ($F(1,9) = 1.795$, $p = .213$) and no interaction effect between the peripherals

of interest and subject group ($F(1,9) = .485$, $p = .504$) for the blue condition. *Post-hoc* independent-sample t-tests between the two subject groups found a significant difference for target color ($t(9) = 5.525$, $p < .001$), where the high performing group (M = 12.99, SD = 1.22) had higher SNR values than the low performing group (M = 7.64, SD = 1.85). There was also a significant difference between the two groups for the blue distractor color ($t(9) = 3.098$, $p = .013$), where the high performing group (M = 12.29, SD = 5.00) had higher SNR values than the low performing group (M = 5.42, SD = 2.03).

For the red condition, there was a main effect for the peripheral colors of interest (target and red distractor) ($F(1,9) = 5.820$, $p = .039$, $\eta^2 = .393$). There was no interaction effect between the peripherals of interest and subject group ($F(1,9) = .015$, $p = .906$) and no significant difference between subject groups ($F(1,9) = 3.898$, $p = .080$) for the red condition. *Post-hoc* independent-sample t-tests between the two subject groups found no significant difference for the target color ($t(9) = 1.571$, $p = .151$) or the red distractor color ($t(9) = 1.937$, $p = .085$).

Figure 22 transforms the SNR values in Figure 21 by subtracting each SNR value from the respective subject's control peripheral, the 180° peripheral stimuli's SNR value in the neutral condition. This transformation is used to visualize attentional enhancement and suppression in relation to the control peripheral's SNR. In both distractor conditions and both subject groups, we observe decreased SNRs in the peripheral colors that match the condition's distractors. The peripheral colors that match condition distractors are the +45° peripheral color in the blue condition and the -45° peripheral color in the red condition. SSVEP responses to peripheral stimuli which are colored to match a distractor are reduced in the red and blue conditions, relative to the neutral condition, with the one exception of the relative SNR for blue distractors in the results for high performers (bottom left plot). Note also that the red distractor condition displayed a large SNR increase for the SSVEP response to the +22.5° peripheral color.

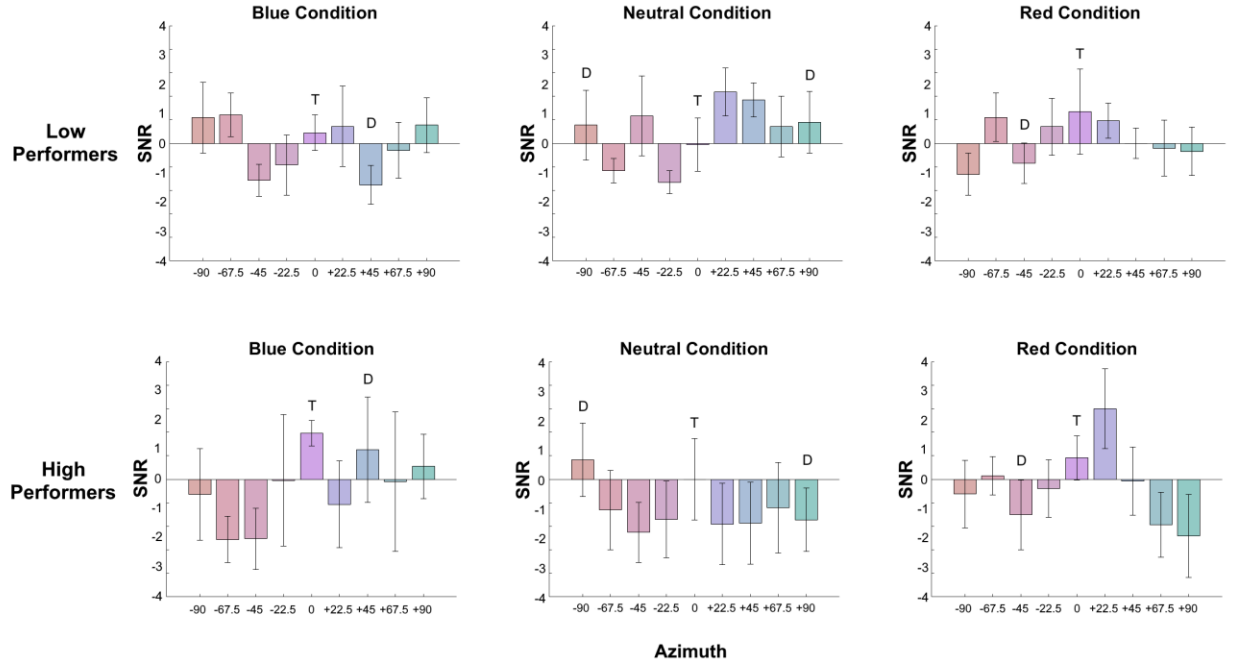

Figure 22. Bar plots displaying relative channel-averaged and participant-averaged SNRs using as baseline each subject's neutral condition response to the 180° peripheral stimulus. These relative SNRs display attentional enhancement and suppression directly. The top row displays the results for the low performers and the bottom row displays the results for the high performers.

4.4 Discussion

The current study examined feature-based attention for color using a visual search task with a purple target and with distractors that shared either the red or the blue coloration of the target. Using blue distractors while searching for purple limits one's ability to use the blue information presented by the purple target, while using red distractors limits one's ability to use the red information presented by the target. We varied the chromatic properties of a flickering peripheral field while participants performed the foveal visual search task. We used EEG to determine the strength of the SSVEP response to the flickering peripheral field while varying field chromatic properties. The strength of the SSVEP responses as a function of peripheral field color are a measure of the chromatic sensitivity of feature-based attention for a particular task. By varying distractor color in the foveal visual search task, we are able to measure how feature-based attention may be varied to enhance the response to a target while minimizing the response to distractors.

Our study found two groups of subjects, high performers and low performers, which displayed significant differences in their behavioral performance of the task. Within each group of subjects and across all subjects, performance in the neutral, blue, and red conditions were similar. In other words, the three conditions were equivalent in terms of task difficulty.

The SSVEPs produced by the peripheral flicker revealed the expected peaks at the peripheral field's flicker frequency of 15 Hz and at the second harmonic 30 Hz. Activity was localized to parietal-occipital cortex. These results agree with those from earlier studies of feature-based attention using peripheral SSVEPs (Chu & D'Zmura, 2019; Hasan et al., 2017; Painter et al., 2014; D. Zhang et al., 2010). This also indicates minimal differences between peripheral stimuli conditions in terms of their ability to produce SSVEPs, thus the observed differences are more likely due to attentional mechanisms related to feature-based attention. This assumption is further supported by previous studies on feature-based attention that have found global enhancement for attended features across the visual field, which have found higher SSVEPs for attended features and lower or unaffected SSVEPs for distractor features (Andersen et al., 2013, 2008; Andersen, Muller, & Hillyard, 2015; Forschack et al., 2017). Previous studies have also found that unattended features that do not directly compete with the target feature for attention are unaffected by this global property of feature-based attention (Forschack et al., 2017; M. M. Müller et al., 2018). As such, the peripheral flicker stimuli colors should not affect the attentional filter being measured from the foveal task.

In the neutral condition, the high performers and low performers exhibited slightly different SNRs. The high performers exhibited a pattern with an increased SNR at the target color and decreased SNRs at the surrounding colors, a similar pattern found in previous psychophysical and neurophysiological studies (Bartsch et al., 2017; Fang, Becker, & Liu, 2019; Geng, DiQuattro, & Helm, 2017; Kehoe, Rahimi, & Fallah, 2018; Störmer & Alvarez, 2014; Tombu & Tsotsos, 2008; Wang et al., 2015; Yoo, Tsotsos, & Fallah, 2018). The low performers seemed to weigh the blue colors higher and the red colors lower. This difference in the neutral condition suggests that the reason the low performers performed poorly on the task compared to the high performers was because the low performers had difficulty isolating the target color purple. While previous studies in feature-based attention have found attentional profiles that decrease with distance from the attended feature, as found with the SNR results of high performers in the

present study, the SNR results of low performers in the present study may indicate that the attentional profile may not follow the previously found pattern if the task is too difficult.

In both distractor conditions, we observed decreases in SSVEP responses for the distractor colored peripherals compared to the target colored peripheral. In the blue condition, the high performing group produced higher SSVEP responses than the low performing group for the target color. Additionally, the high performing subjects during the red distractor condition produced significantly higher SSVEP responses for the distractor color compared to the low performing subjects; we also note an interesting enhancement of the +22.5° peripheral, slightly further away from the distractor color, that is higher than the target colored peripheral. This could indicate a shift in the attentional selection profile toward blue that helps high performing subjects to better select the target color in the presence of red distractors. This effect did not appear in the blue distractor condition for high performers, so the results seem mixed. However, it is possible that the target purple color chosen may have appeared more red than blue, which may explain the general bias in the results away from the red peripheral colors. Previous studies have found that subjective appearance of color category influence attentional selection and that there may be different attentional profiles for different color categories (Daoutis et al., 2006; Fang et al., 2019; Jiang et al., 2017). This effect of color category may have influenced the attentional profiles observed in the distractor conditions, and future studies could examine the attentional profiles for other target-distractor color combinations.

While the current study found differences between subject ability to perform the visual search task, future studies could incorporate a process to set individual difficulty levels for the task to control for individual differences. This would allow us to control for task difficulty and observe more directly if the differences in attentional mechanisms examined in the current study arose due to different strategies in relation to task difficulty. Additionally, since all the conditions in the current study were linearly separable, a future study could also incorporate a non-linearly separable condition. If one of the conditions were non-linearly separable, then we would expect there to be a large increase in performance difficulty compared to the linearly separable conditions. The resulting attentional profile exhibited through SSVEP responses would be expected to peak more highly at the target color compared to the neutral condition in a non-linearly separable condition.

4.5 Conclusion

In conclusion, the present study examined the attentional profile of feature-based attention for color by measuring SSVEP responses to flickering peripheral chromatic stimuli while subjects performed foveal color search tasks. We examined the attentional profile for distractors that had minimal effect on detecting the purple target, distractors that influenced the use of blue information carried by the target, and distractors that influenced the use of red information carried by the target. SSVEP signal-to-noise ratios showed that there are smaller responses for the distractor colors in the blue and red distractor conditions. These results suggest that feature-based attention to a particular color involves chromatic mechanisms that both enhance the response to a target and minimize responses to distractors.

5 References

Ambadar, Z., Cohn, J. F., & Reed, L. I. (2009). All Smiles are Not Created Equal: Morphology and Timing of Smiles Perceived as Amused, Polite, and Embarrassed/Nervous. *Journal of Nonverbal Behavior*, *33*(1), 17–34. https://doi.org/10.1007/s10919-008-0059-5

Andersen, S. K., Fuchs, S., & Müller, M. M. (2011). Effects of Feature-selective and Spatial Attention at Different Stages of Visual Processing. *Journal of Cognitive Neuroscience*, *23*(1), 238–246. https://doi.org/10.1162/jocn.2009.21328

Andersen, S. K., Hillyard, S. A., & Muller, M. M. (2013). Global Facilitation of Attended Features Is Obligatory and Restricts Divided Attention. *Journal of Neuroscience*, *33*(46), 18200–18207. https://doi.org/10.1523/JNEUROSCI.1913-13.2013

Andersen, S. K., Hillyard, S. A., & Müller, M. M. (2008). Attention Facilitates Multiple Stimulus Features in Parallel in Human Visual Cortex. *Current Biology*, *18*(13), 1006–1009. https://doi.org/10.1016/j.cub.2008.06.030

Andersen, S. K., Muller, M. M., & Hillyard, S. A. (2009). Color-selective attention need not be mediated by spatial attention. *Journal of Vision*, *9*(6), 1–7. https://doi.org/10.1167/9.6.2

Andersen, S. K., Muller, M. M., & Hillyard, S. A. (2015). Attentional Selection of Feature Conjunctions Is Accomplished by Parallel and Independent Selection of Single Features. *Journal of Neuroscience*, *35*(27), 9912–9919. https://doi.org/10.1523/JNEUROSCI.5268-14.2015

Andersen, S. K., Muller, M. M., & Martinovic, J. (2012). Bottom-Up Biases in Feature-Selective Attention. *Journal of Neuroscience*, *32*(47), 16953–16958. https://doi.org/10.1523/JNEUROSCI.1767-12.2012

Baltrušaitis, T., Robinson, P., & Morency, L. P. (2016). Openface: an open source facial behavior analysis toolkit. In *2016 IEEE Winter Conference on Applications of Computer Vision (WACV)*. Lake Placid, NY, USA: IEEE. https://doi.org/10.1109/WACV.2016.7477553

Bartsch, M. V., Loewe, K., Merkel, C., Heinze, H.-J., Schoenfeld, M. A., Tsotsos, J. K., & Hopf, J.-M. (2017). Attention to color sharpens neural population tuning via feedback processing

in the human visual cortex hierarchy. *Journal of Neuroscience*, *37*(43), 10346–10357. https://doi.org/10.1523/JNEUROSCI.0666-17.2017

Bauer, B., Jolicoeur, P., & Cowan, W. B. (1996a). Linear separability in colour visual search. *Perception*, *25*, 1281–1293. https://doi.org/10.1068/p251281

Bauer, B., Jolicoeur, P., & Cowan, W. B. (1996b). Visual search for colour targets that are or are not linearly separable from distractors. *Vision Research*, *36*(10), 1439–1466. https://doi.org/10.1016/0042-6989(95)00207-3

Bauer, B., Jolicoeur, P., & Cowan, W. B. (1998). The linear separability effect in color visual search: Ruling out the additive color hypothesis. *Perception & Psychophysics*, *60*(6), 1083–1093. https://doi.org/10.3758/BF03211941

Bauer, B., Jolicoeur, P., & Cowan, W. B. (1999). Convex hull test of the linear separability hypothesis in visual search. *Vision Research*, *39*, 2681–2695. https://doi.org/10.1016/S0042-6989(98)00302-2

Berkebile, B. (2010). iTween for Unity. Retrieved from http://www.pixelplacement.com/itween/index.php

Blascovich, J. (2008). Challenge and Threat. In A. J. Elliot (Ed.), *Handbook of Approach and Avoidance Motivation* (pp. 431–445). New York, NY, USA: Psychology Press. https://doi.org/10.4324/9780203888148.ch25

Blascovich, J., Mendes, W. B., Hunter, S. B., Lickel, B., & Kowai-Bell, N. (2001). Perceiver threat in social interactions with stigmatized others. *Journal of Personality and Social Psychology*, *80*(2), 253–267. https://doi.org/10.1037/0022-3514.80.2.253

Blascovich, J., Mendes, W. B., Hunter, S. B., & Salomon, K. (1999). Social "facilitation" as challenge and threat. *Journal of Personality and Social Psychology*, *77*(1), 68–77. https://doi.org/10.1037/0022-3514.77.1.68

Blascovich, J., Mendes, W. B., & Seery, M. D. (2002). Intergroup Encounters and Threat: A Multi-Method Approach. In D. Mackie & E. Smith (Eds.), *From prejudice to intergroup emotions: Differentiated reactions to social groups* (pp. 88–109). New York, NY, USA: Psychology Press.

Blascovich, J., & Seery, M. D. (2007). Visceral and somatic indices of social psychological constructs. In A. Kruglanski & E. T. Higgins (Eds.), *Social Psychology: Handbook of Basic Principles* (2nd ed., pp. 19–38). New York, NY, USA: Guilford Press.

Blascovich, J., Seery, M. D., Mugridge, C. A., Norris, R. K., & Weisbuch, M. (2004). Predicting athletic performance from cardiovascular indexes of challenge and threat. *Journal of Experimental Social Psychology*, *40*(5), 683–688. https://doi.org/10.1016/j.jesp.2003.10.007

Bridwell, D. A., & Srinivasan, R. (2012). Distinct Attention Networks for Feature Enhancement and Suppression in Vision. *Psychological Science*, *23*(10), 1151–1158. https://doi.org/10.1177/0956797612440099

Brunner, C., Allison, B. Z., Altstätter, C., & Neuper, C. (2011). A comparison of three brain-computer interfaces based on event-related desynchronization, steady state visual evoked potentials, or a hybrid approach using both signals. *Journal of Neural Engineering*, *8*(2). https://doi.org/10.1088/1741-2560/8/2/025010

Calore, E., Gadia, D., & Marini, D. (2014). Eliciting steady-state visual evoked potentials by means of stereoscopic displays. In *Stereoscopic Displays and Applications XXV* (p. 901126). https://doi.org/10.1117/12.2036936

Cao, T., Wan, F., Wong, C. M., da Cruz, J. N., & Hu, Y. (2014). Objective evaluation of fatigue by EEG spectral analysis in steady-state visual evoked potential-based brain-computer interfaces. *BioMedical Engineering Online*, *13*(1), 1–13. https://doi.org/10.1186/1475-925X-13-28

Caputo, G., & Guerra, S. (1998). Attentional Selection by Distractor Suppression. *Vision Research*, *38*(5), 669–689. https://doi.org/10.1016/S0042-6989(97)00189-2

Cecotti, H., & Ries, A. J. (2017). Best practice for single-trial detection of event-related potentials: Application to brain-computer interfaces. *International Journal of Psychophysiology*, *111*, 156–169. https://doi.org/10.1016/j.ijpsycho.2016.07.500

Chu, V. C., & D'Zmura, M. (2019). Tracking feature-based attention. *Journal of Neural Engineering*, *16*(1). https://doi.org/10.1088/1741-2552/aaed17

Cieslak, M. (2016). *Dynamics of the central and autonomic nervous systems preceding action*

and cognition. University of California, Santa Barbara.

Cieslak, M., Ryan, W. S., Babenko, V., Erro, H., Rathbun, Z. M., Meiring, W., … Grafton, S. T. (2018). Quantifying rapid changes in cardiovascular state with a moving ensemble average. *Psychophysiology*, *55*(4), 1–17. https://doi.org/10.1111/psyp.13018

Cobb, S. V. G., Nichols, S., Ramsey, A., & Wilson, J. R. (1999). Virtual reality-induced symptoms and effects (VRISE). *Presence*, *8*(2), 169–186. https://doi.org/10.1086/250095

D'Zmura, M. (1991). Color in visual search. *Vision Research*, *31*(6), 951–966. https://doi.org/10.1016/0042-6989(91)90203-H

Daoutis, C. A., Pilling, M., & Davies, I. R. L. (2006). Categorical effects in visual search for colour. *Visual Cognition*, *14*(2), 217–240. https://doi.org/10.1080/13506280500158670

de Melo, C. M., Carnevale, P. J., Read, S. J., & Gratch, J. (2014). Reading people's minds from emotion expressions in interdependent decision making. *Journal of Personality and Social Psychology*, *106*(1), 73–88. https://doi.org/10.1037/a0034251

Dennison, M. S., Wisti, A. Z., & D'Zmura, M. (2016). Use of physiological signals to predict cybersickness. *Displays*, *44*, 42–52. https://doi.org/10.1016/j.displa.2016.07.002

Derrington, A. M., Krauskopf, J., & Lennie, P. (1984). Chromatic mechanisms in lateral geniculate nucleus of macaque. *Journal of Physiology1*, *357*(1), 241–265. https://doi.org/10.1113/jphysiol.1984.sp015499

Dienstbier, R. A. (1989). Arousal and Physiological Toughness: Implications for Mental and Physical Health. *Psychological Review*, *96*(1), 84–100. https://doi.org/10.1037/0033-295X.96.1.84

Duncan, J., & Humphreys, G. W. (1989). Visual Search and Stimulus Similarity. *Psychological Review*, *96*(3), 433–458. https://doi.org/10.1037/0033-295X.96.3.433

Dunn, J. R., & Schweitzer, M. E. (2005). Feeling and believing: The influence of emotion on trust. *Journal of Personality and Social Psychology*, *88*(5), 736–748. https://doi.org/10.1037/0022-3514.88.5.736

Ekman, P., Friese, W., & Davidson, R. (1988). The Duchenne Smile: Emotional Expression And

Brain Physiology II. *Journal of Personality and Social Psychology*, *58*(2), 342–353.

Eriksen, C. W., & St. James, J. D. (1986). Visual attention witnin and around the field of focal attention: A zoom lens model. *Perception and Psychophysics*, *40*(4), 225–240. https://doi.org/10.3758/BF03211502

Fabiansson, E. C., & Denson, T. F. (2012). The Effects of Intrapersonal Anger and Its Regulation in Economic Bargaining. *PLoS ONE*, *7*(12). https://doi.org/10.1371/journal.pone.0051595

Fang, M. W. H., Becker, M. W., & Liu, T. (2019). Attention to colors induces surround suppression at category boundaries. *Scientific Reports*, *9*(1), 1–13. https://doi.org/10.1038/s41598-018-37610-7

Faul, F., Erdfelder, E., Lang, A.-G., & Buchner, A. (2007). G*Power 3: a flexible statistical power analysis program for the social, behavioral, and biomedical sciences. *Behavior Research Methods*, *39*(2), 175–191. https://doi.org/10.3758/BF03193146

Fazel-Rezai, R., Allison, B. Z., Guger, C., Sellers, E. W., Kleih, S. C., & Kübler, A. (2012). P300 brain computer interface: current challenges and emerging trends. *Frontiers in Neuroengineering*, *5*(July), 1–14. https://doi.org/10.3389/fneng.2012.00014

Fehr, E., & Gächter, S. (2002). Altruistic punishment in humans. *Nature*, *415*(6868), 137–140. https://doi.org/10.1038/415137a

Feinberg, M., Willer, R., Antonenko, O., & John, O. P. (2012). Liberating Reason From the Passions: Overriding Intuitionist Moral Judgments Through Emotion Reappraisal. *Psychological Science*, *23*(7), 788–795. https://doi.org/10.1177/0956797611434747

Forschack, N., Andersen, S. K., & Muller, M. M. (2017). Global Enhancement but Local Suppression in Feature-based Attention. *Journal of Cognitive Neuroscience*, *29*(4), 619–627. https://doi.org/10.1162/jocn_a_01075

Geng, J. J., DiQuattro, N. E., & Helm, J. (2017). Distractor probability changes the shape of the attentional template. *Journal of Experimental Psychology: Human Perception and Performance*. https://doi.org/10.1037/xhp0000430

Grecucci, A., Giorgetta, C., Bonini, N., & Sanfey, A. G. (2013). Living emotions, avoiding emotions: Behavioral investigation of the regulation of socially driven emotions. *Frontiers in Psychology*, *3*, 1–14. https://doi.org/10.3389/fpsyg.2012.00616

Grecucci, A., Giorgetta, C., Van't Wout, M., Bonini, N., & Sanfey, A. G. (2013). Reappraising the ultimatum: An fMRI study of emotion regulation and decision making. *Cerebral Cortex*, *23*(2), 399–410. https://doi.org/10.1093/cercor/bhs028

Gross, J. J. (1999). Emotion regulation: Past, present, future. *Cognition and Emotion*, *13*(5), 551–573. https://doi.org/10.1080/026999399379186

Gross, J. J. (2002). Emotion regulation: affective, cognitive, and social consequences. *Psychophysiology*, *39*(3), 281–291. https://doi.org/10.1017.S0048577201393198

Gross, J. J., & John, O. P. (2003). Individual differences in two emotion regulation processes: implications for affect, relationships, and well-being. *Journal of Personality and Social Psychology*, *85*(2), 348–362. https://doi.org/10.1037/0022-3514.85.2.348

Guger, C., Daban, S., Sellers, E., Holzner, C., Krausz, G., Carabalona, R., … Edlinger, G. (2009). How many people are able to control a P300-based brain-computer interface (BCI)? *Neuroscience Letters*, *462*(1), 94–98. https://doi.org/10.1016/j.neulet.2009.06.045

Hasan, R., Grossman, E. D., & Srinivasan, R. (2017). Feature-based attentional tuning during biological motion detection measured with SSVEP. *Journal of Vision*, *17*(9), 1–12. https://doi.org/10.1167/17.9.22.doi

Hodsoll, J. L., & Humphreys, G. W. (2001). Driving attention with the top down: The relative contribution of target templates to the linear separability effect in the size dimension. *Perception and Psychophysics*, *63*(5), 918–926. https://doi.org/10.3758/BF03194447

Hopf, J.-M., Boelmans, K., Schoenfeld, M. A., Luck, S. J., & Heinze, H.-J. (2004). Attention to Features Precedes Attention to Locations in Visual Search: Evidence from Electromagnetic Brain Responses in Humans. *Journal of Neuroscience*, *24*(8), 1822–1832. https://doi.org/10.1523/JNEUROSCI.3564-03.2004

Jamieson, J. P., Mendes, W. B., & Nock, M. K. (2013). Improving Acute Stress Responses: The Power of Reappraisal. *Current Directions in Psychological Science*, *22*(1), 51–56.

https://doi.org/10.1177/0963721412461500

Jamieson, J. P., Nock, M. K., & Mendes, W. B. (2012). Mind over matter: Reappraising arousal improves cardiovascular and cognitive responses to stress. *Journal of Experimental Psychology: General*, *141*(3), 417–422. https://doi.org/10.1037/a0025719

Jiang, Y., Wu, X., & Gao, X. (2017). A category-specific top-down attentional set can affect the neural responses outside the current focus of attention. *Neuroscience Letters*, *659*, 80–85. https://doi.org/10.1016/j.neulet.2017.07.029

Kehoe, D. H., Rahimi, M., & Fallah, M. (2018). Perceptual color space representations in the oculomotor system are modulated by surround suppression and biased selection. *Frontiers in Systems Neuroscience*, *12*(January). https://doi.org/10.3389/fnsys.2018.00001

Kennedy, R. S., Lane, N. E., Berbaum, K. S., & Lilienthal, M. G. (1993). Simulator Sickness Questionnaire : An Enhanced Method for Quantifying Simulator Sickness. *The International Journal of Aviation Psychology*, *3*(3), 203–220. https://doi.org/10.1207/s15327108ijap0303

Khooshabeh, P., de Melo, C. M., Volkman, B., Gratch, J., Blascovich, J., & Carnevale, P. J. (2013). Negotiation Strategies with Incongruent Facial Expressions of Emotion Cause Cardiovascular Threat. In *Proceedings of the 35th Annual Meeting of the Cognitive Science Society* (pp. 770–775). Berlin, Germany.

Khooshabeh, P., Lin, R., de Melo, C., Gratch, J., Ouimette, B., & Blascovich, J. (2016). Neurophysiological Effects of Negotiation Framing. In *Proceedings of the 38th Annual Conference of the Cognitive Science Society* (pp. 2369–2374). Austin, Texas.

Krumhuber, E., Manstead, A. S. R., & Kappas, A. (2007). Temporal aspects of facial displays in person and expression perception: The effects of smile dynamics, head-tilt, and gender. *Journal of Nonverbal Behavior*, *31*(1), 39–56. https://doi.org/10.1007/s10919-006-0019-x

Krusienski, D. J., Sellers, E. W., Cabestaing, F., Bayoudh, S., Mcfarland, D. J., Vaughan, T. M., & Wolpaw, J. R. (2010). A comparison of classification techniques for the P300 speller. *Journal of Neural Engineering*, *3*(4), 299–305. https://doi.org/10.1088/1741-2560/3/4/007

Kunić, S., & Šego, Z. (2012). OLED Technology and Displays. In *2012 Proceedings ELMAR*

(pp. 12–14). Zadar, Croatia: IEEE.

Lalor, E. C., Kelly, S. P., Finucane, C., Burke, R., Smith, R., Reilly, R. B., & McDarby, G. (2005). Steady-State VEP-based brain-computer interface control in an immersive 3D gaming environment. In *EURASIP Journal on Applied Signal Processing Journal on Applied Signal Processing* (Vol. 19, pp. 3156–3164). https://doi.org/10.1155/ASP.2005.3156

Lee, B. B., Martin, P. R., & Valberg, A. (1988). The physiological basis of heterochromatic flicker photometry demonstrated in the ganglion cells of the macaque retina. *Journal of Physiology*, *404*(1), 323–347. https://doi.org/10.1113/jphysiol.1988.sp017292

Leonard, C. J., Balestreri, A., & Luck, S. J. (2015). Interactions between space-based and feature-based attention. *Journal of Experimental Psychology: Human Perception and Performance*, *41*(1), 11–16. https://doi.org/10.1037/xhp0000011

Lerner, J. S., & Tiedens, L. Z. (2006). Portrait of the angry decision maker: How appraisal tendencies shape Anger's influence on cognition. *Journal of Behavioral Decision Making*, *19*(2), 115–137. https://doi.org/10.1002/bdm.515

Lin, F.-C., Zao, J. K., Tu, K.-C., Wang, Y., Huang, Y.-P., Chuang, C.-W., … Jung, T.-P. (2012). An SNR Analysis of High-Frequency Steady-State Visual Evoked Potentials from the Foveal and Extrafoveal Regions of Human Retina. In *2012 Annual International Conference of the IEEE Engineering in Medicine and Biology Society (EMBC)* (pp. 1810–1814). San Diego, CA: IEEE. https://doi.org/10.1109/EMBC.2012.6346302

Liu, T., Larsson, J., & Carrasco, M. (2007). Feature-Based Attention Modulates Orientation-Selective Responses in Human Visual Cortex. *Neuron*, *55*(2), 313–323. https://doi.org/10.1016/j.neuron.2007.06.030

Liu, T., & Mance, I. (2011). Constant spread of feature-based attention across the visual field. *Vision Research*, *51*(1), 26–33. https://doi.org/10.1016/j.visres.2010.09.023

McCauley, M. E., & Sharkey, T. J. (1993). Cybersickness : Perception of Self-Motion in Virtual Environments. *Presence*, *1*(3), 311–318. https://doi.org/10.1162/pres.1992.1.3.311

Mendes, W. B., Blascovich, J., Lickel, B., & Hunter, S. (2002). Challenge and threat during

social interactions with White and Black men. *Personality and Social Psychology Bulletin*, *28*(7), 939–952. https://doi.org/10.1177/01467202028007007

Mendes, W. B., Major, B., McCoy, S., & Blascovich, J. (2008). How Attributional Ambiguity Shapes Physiological and Emotional Responses to Social Rejection and Acceptance. *Journal of Personality and Social Psychology*, *94*(2), 278–291. https://doi.org/10.1037/0022-3514.94.2.278

Moher, J., Lakshmanan, B. M., Egeth, H. E., & Ewen, J. B. (2014). Inhibition Drives Early Feature-Based Attention. *Psychological Science*, *25*(2), 315–324. https://doi.org/10.1177/0956797613511257

Morgan, S. T., Hansen, J. C., & Hillyard, S. A. (1996). Selective attention to stimulus location modulates the steady-state visual evoked potential. *Proceedings of the National Academy of Sciences*, *93*(10), 4770–4774. https://doi.org/10.1073/pnas.93.10.4770

Motter, B. C. (1994). Neural Correlates of Attentive Selection for Color or Luminance in Extrastriate Area V4. *The Journal of Neuroscience*, *14*(4), 2178–2189.

Muller, M. M., Andersen, S. K., Trujillo, N. J., Valdes-Sosa, P., Malinowski, P., & Hillyard, S. A. (2006). Feature-selective attention enhances color signals in early visual areas of the human brain. *Proceedings of the National Academy of Sciences*, *103*(38), 14250–14254. https://doi.org/10.1073/pnas.0606668103

Müller, M. M., Gundlach, C., Forschack, N., & Brummerloh, B. (2018). It takes two to tango: Suppression of task-irrelevant features requires (spatial) competition. *NeuroImage*, *178*, 485–492. https://doi.org/10.1016/j.neuroimage.2018.05.073

Müller, N. G., Bartelt, O. A., Donner, T. H., Villringer, A., & Brandt, S. A. (2003). A physiological correlate of the "Zoom Lens" of visual attention. *The Journal of Neuroscience*, *23*(9), 3561–3565. Retrieved from http://www.ncbi.nlm.nih.gov/entrez/query.fcgi?cmd=Retrieve&db=PubMed&dopt=Citation&list_uids=12736325

Mun, S., Cho, S., Whang, M., Ju, B.-K., & Park, M.-C. (2012). SSVEP-based BCI for manipulating three-dimensional contents and devices. In *Proc. SPIE 8384, Three-*

Dimensional Imaging, Visualization, and Display 2012 (p. 83840T). https://doi.org/10.1117/12.921445

Mun, S., Park, M. C., Park, S., & Whang, M. (2012). SSVEP and ERP measurement of cognitive fatigue caused by stereoscopic 3D. *Neuroscience Letters*, *525*(2), 89–94. https://doi.org/10.1016/j.neulet.2012.07.049

Nagy, A. L., & Sanchez, R. R. (1990). Critical color differences determined with a visual search task. *Journal of the Optical Society of America A*, *7*(7), 1209–1217. https://doi.org/10.1364/josaa.7.001209

Ng, K. B., Bradley, A. P., & Cunnington, R. (2012). Stimulus specificity of a steady-state visual-evoked potential-based brain-computer interface. *Journal of Neural Engineering*, *9*(3). https://doi.org/10.1088/1741-2560/9/3/036008

Nicolas-Alonso, L. F., & Gomez-Gil, J. (2012). Brain computer interfaces, a review. *Sensors*, *12*(2), 1211–1279. https://doi.org/10.3390/s120201211

Nobre, A. C., Sebestyen, G. N., & Miniussi, C. M. (2000). The dynamics of shifting visuospatial attention revealed by event-related potentials. *Neuropsychologia*, *38*, 964–974. https://doi.org/10.1016/S0028-3932(00)00015-4

Norcia, A. M., Appelbaum, L. G., Ales, J. M., Cottereau, B. R., & Rossion, B. (2015). The steady-state visual evoked potential in vision research: A review. *Journal of Vision*, *15*(6), 4. https://doi.org/10.1167/15.6.4.doi

Nunez, M. D., Vandekerckhove, J., & Srinivasan, R. (2017). How attention influences perceptual decision making: Single-trial EEG correlates of drift-diffusion model parameters. *Journal of Mathematical Psychology*, *76*, 117–130. https://doi.org/10.1016/j.jmp.2016.03.003

Painter, D. R., Dux, P. E., & Mattingley, J. B. (2015). Causal involvement of visual area MT in global feature-based enhancement but not contingent attentional capture. *NeuroImage*, *118*, 90–102. https://doi.org/10.1016/j.neuroimage.2015.06.019

Painter, D. R., Dux, P. E., Travis, S. L., & Mattingley, J. B. (2014). Neural Responses to Target Features outside a Search Array Are Enhanced during Conjunction but Not Unique-Feature Search. *Journal of Neuroscience*, *34*(9), 3390–3401.

https://doi.org/10.1523/JNEUROSCI.3630-13.2014

Posner, M. I. (1980). Orienting of attention. *The Quarterly Journal of Experimental Psychology*, *32*(1), 3–25. https://doi.org/10.1080/00335558008248231

Poundstone, W. (1993). *Prisoner's Dilemma: John von Neumann, Game Theory, and the Puzzle*. USA: Anchor.

Reed, L. I., Zeglen, K. N., & Schmidt, K. L. (2012). Facial expressions as honest signals of cooperative intent in a one-shot anonymous Prisoner's Dilemma game. *Evolution and Human Behavior*, *33*(3), 200–209. https://doi.org/10.1016/j.evolhumbehav.2011.09.003

Riccio, A., Mattia, D., Simione, L., Olivetti, M., & Cincotti, F. (2012). Eye-gaze independent EEG-based brain-computer interfaces for communication. *Journal of Neural Engineering*, *9*(4). https://doi.org/10.1088/1741-2560/9/4/045001

Rousselet, G. A., Fabre-Thorpe, M., & Thorpe, S. J. (2002). Parallel processing in high-level categorization of natural images. *Nature Neuroscience*, *5*(7), 629–630. https://doi.org/10.1038/nn866

Saenz, M., Buracas, G. T., & Boynton, G. M. (2002). Global effects of feature-based attention in human visual cortex. *Nature Neuroscience*, *5*(7), 631–632. https://doi.org/10.1038/nn876

Seery, M. D. (2013). The Biopsychosocial Model of Challenge and Threat: Using the Heart to Measure the Mind. *Social and Personality Psychology Compass*, *7*(9), 637–653. https://doi.org/10.1111/spc3.12052

Seery, M. D., Blascovich, J., Weisbuch, M., & Vick, S. B. (2004). The relationship between self-esteem level, self-esteem stability, and cardiovascular reactions to performance feedback. *Journal of Personality and Social Psychology*, *87*(1), 133–145. https://doi.org/10.1037/0022-3514.87.1.133

Serences, J. T., & Boynton, G. M. (2007). Feature-Based Attentional Modulations in the Absence of Direct Visual Stimulation. *Neuron*, *55*(2), 301–312. https://doi.org/10.1016/j.neuron.2007.06.015

Srinivasan, R., Bibi, F. A., & Nunez, P. L. (2006). Steady-state visual evoked potentials:

Distributed local sources and wave-like dynamics are sensitive to flicker frequency. *Brain Topography*, *18*(3), 167–187. https://doi.org/10.1007/s10548-006-0267-4

Störmer, V. S., & Alvarez, G. A. (2014). Feature-based attention elicits surround suppression in feature space. *Current Biology*, *24*(17), 1985–1988. https://doi.org/10.1016/j.cub.2014.07.030

Stratou, G., Hoegen, R., Lucas, G., & Gratch, J. (2015). Emotional signaling in a social dilemma: An automatic analysis. In *2015 International Conference on Affective Computing and Intelligent Interaction, ACII 2015* (pp. 180–186). Xi'an, China: IEEE. https://doi.org/10.1109/ACII.2015.7344569

Sun, P., Chubb, C., Wright, C. E., & Sperling, G. (2016). Human attention filters for single colors. *Proceedings of the National Academy of Sciences*, *113*(43), E6712–E6720. https://doi.org/10.1073/pnas.1614062113

Tombu, M., & Tsotsos, J. K. (2008). Attending to orientation results in an inhibitory surround in orientation space. *Perception & Psychophysics*, *70*(1), 30–35. https://doi.org/10.3758/PP.70.1.30

Tonin, L., Leeb, R., & Millán, J. del R. (2012). Time-dependent approach for single trial classification of covert visuospatial attention. *Journal of Neural Engineering*, *9*(4). https://doi.org/10.1088/1741-2560/9/4/045011

Treder, M. S., Schmidt, N. M., & Blankertz, B. (2011). Gaze-independent brain-computer interfaces based on covert attention and feature attention. *Journal of Neural Engineering*, *8*(6), 1–12. https://doi.org/10.1088/1741-2560/8/6/066003

Treisman, A. M., & Gelade, G. (1980). A Feature-Integration Theory of Attention. *Cognitive Psychology*, *12*, 97–136. https://doi.org/10.1016/0010-0285(80)90005-5

Treue, S., & Trujillo, J. C. M. (1999). Feature-based attention influences motion processing gain in macaque visual cortex. *Nature*, *399*, 575–579. https://doi.org/10.1038/21176

VanRullen, R., & Thorpe, S. J. (2001). The Time Course of Visual Processing: From Early Perception to Decision-Making. *Journal of Cognitive Neuroscience*, *13*(4), 454–461. https://doi.org/10.1162/08989290152001880

Vauderwange, O., Curticapean, D., Dreßler, P., & Wozniak, P. (2014). Digital devices: Big challenge in color management. In G. G. Gregory (Ed.), *Proc. SPIE 9188, Optics Education and Outreach III* (p. 91880B). San Diego, CA: SPIE. https://doi.org/10.1117/12.2061885

Wan, F., Da Cruz, J. N., Nan, W., Wong, C. M., Vai, M. I., & Rosa, A. (2016). Alpha neurofeedback training improves SSVEP-based BCI performance. *Journal of Neural Engineering*, *13*(3). https://doi.org/10.1088/1741-2560/13/3/036019

Wang, Y., Miller, J., & Liu, T. (2015). Suppression effects in feature-based attention. *Journal of Vision*, *15*(5), 1–16. https://doi.org/10.1167/15.5.15

Wittenburg, P., Brugman, H., Russel, A., Klassmann, A., & Sloetjes, H. (2006). ELAN: A professional framework for multimodality research. In *Proceedings Language Resources and Evaluation* (pp. 1556–1559). https://doi.org/10.3758/BRM.41.3.591

Wolfe, J. M. (1994). Guided Search 2.0: A revised model of visual search. *Psychnomic Bulletin & Review*, *1*(2), 202–238. https://doi.org/10.3758/BF03200774

Won, D.-O., Hwang, H.-J., Dähne, S., Müller, K.-R., & Lee, S.-W. (2016). Effect of higher frequency on the classification of steady-state visual evoked potentials. *Journal of Neural Engineering*, *13*(1), 016014. https://doi.org/10.1088/1741-2560/13/1/016014

Xie, J., Xu, G., Wang, J., Li, M., Han, C., & Jia, Y. (2016). Effects of mental load and fatigue on steady-state evoked potential based brain computer interface tasks: A comparison of periodic flickering and motion-reversal based visual attention. *PLoS ONE*, *11*(9), 1–15. https://doi.org/10.1371/journal.pone.0163426

Yoo, S.-A., Tsotsos, J. K., & Fallah, M. (2018). The Attentional Suppressive Surround: Eccentricity, Location-Based and Feature-Based Effects and Interactions. *Frontiers in Neuroscience*, *12*(October), 1–14. https://doi.org/10.3389/fnins.2018.00710

Zhang, D., Maye, A., Gao, X., Hong, B., Engel, A. K., & Gao, S. (2010). An independent brain-computer interface using covert non-spatial visual selective attention. *Journal of Neural Engineering*, *7*(1). https://doi.org/10.1088/1741-2560/7/1/016010

Zhang, S., Han, X., Chen, X., Wang, Y., Gao, S., & Gao, X. (2018). A study on dynamic model of steady-state visual evoked potentials. *Journal of Neural Engineering*, *15*.

https://doi.org/10.1088/1741-2552/aabb82

Zhang, W., & Luck, S. J. (2009). Feature-based attention modulates feedforward visual processing. *Nature Neuroscience*, *12*(1), 24–25. https://doi.org/10.1038/nn.2223